MODELLED TARGET STRENGTHS OF THREE LANTERNFISH (FAMILY: MYCTOPHIDAE) IN THE NORTH EAST ATLANTIC BASED ON SWIMBLADDER AND BODY MORPHOLOGY

Birkir Bardarson

A Thesis Submitted for the Degree of MPhil
at the
University of St Andrews

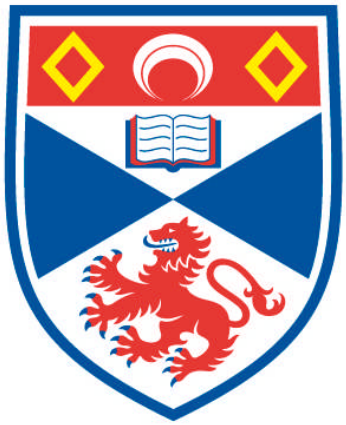

2014

Full metadata for this item is available in
Research@StAndrews:FullText
at:
http://research-repository.st-andrews.ac.uk/

Please use this identifier to cite or link to this item:
http://hdl.handle.net/10023/6607

This item is protected by original copyright

Modelled Target Strengths of three lanternfish (Family: Myctophidae) in the north east Atlantic based on swimbladder and body morphology

Birkir Bardarson

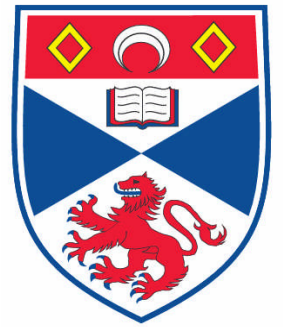

This thesis is submitted in partial fulfilment for the degree of MPhil

at the

University of St Andrews

September 2013

Declarations:

I, Birkir Bardarson, hereby certify that this thesis, which is approximately 17000 words in length, has been written by me, that it is the record of work carried out by me and that it has not been submitted in any previous application for a higher degree.

I was admitted as a research student in January 2004 and as a candidate for the degree of MPhil in April 2005; the higher study for which this is a record was carried out in the University of St Andrews between 2004 and 2008.

Date *11/08/2014* signature of candidate ……..

I hereby certify that the candidate has fulfilled the conditions of the Resolution and Regulations appropriate for the degree of MPhil in the University of St Andrews and that the candidate is qualified to submit this thesis in application for that degree.

Date *11/08/2014* signature of supervisor ……..

Permission for publication:

In submitting this thesis to the University of St Andrews I understand that I am giving permission for it to be made available for use in accordance with the regulations of the University Library for the time being in force, subject to any copyright vested in the work not being affected thereby. I also understand that the title and the abstract will be published, and that a copy of the work may be made and supplied to any bona fide library or research worker, that my thesis will be electronically accessible for personal or research use unless exempt by award of an embargo as requested below, and that the library has the right to migrate my thesis into new electronic forms as required to ensure continued access to the thesis. I have obtained any third-party copyright permissions that may be required in order to allow such access and migration, or have requested the appropriate embargo below.

The following is an agreed request by candidate and supervisor regarding the electronic publication of this thesis:

Access to printed copy and electronic publication of thesis through the University of St Andrews.

Date *11/08/2014* signature of candidate ……..

Date *11/08/2014* signature of supervisor ……..

Table of context

TABLE OF FIGURES

ABSTRACT

At mesopelagic depths (200-1000 m), in the oceanic parts of the earth, there are probably the most abundant fish assemblages in the world, often observed on echosounder displays as sound scattering layers extending over vast areas. Lanternfish are believed to be an important part of those layers. In recent years, acoustic backscatter has been used successfully to quantify pelagic fish stocks, where knowledge of individual fish backscatter proportion, the target strength, is essential for reliable estimate. More knowledge on target strength of the lanternfish found in the Northeast Atlantic is needed before they can be properly identified and quantified by acoustics. Air in the swimbladder will cause much stronger backscatter than the fish body. In this study, external morphology and swimbladder morphology of three abundant lanternfish species *(Benthosema glaciale, Notoscopelus kroeyerii and Myctophum punctatum)* were measured using digital imaging and soft x-ray technology to inform theoretical acoustic target strength (TS) models. The soft x-ray measurements indicated that 71% by number of the adult *B. glaciale* population (sample size (n) = 85) had an air filled swimbladder, while *N. kroeyrii* (n = 127) and *M. punctatum* (n = 99) did not have inflated swimbladders in their adult stage. A distorted wave Born approximation (DWBA) model was used to estimate TS contribution of the fish body while a prolate spheroid resonance scattering model was used for contribution of swimbladder. Further, a comparison was made with exact solution models. At 38 kHz, the commonly used frequency in scientific surveys, *N. kroeyri* was estimated with the TS length relationship of 22.6 log(SL) – 92.8 while *M. punctatum* had 10.9 log(SL) – 81.5. At same frequency the mean TS of B. glaciale was estimated as -64.29 dB with 95% confidence limits of -65.52 and -63.33 dB. Further the TS estimates and scattering properties of all three species were estimated at different frequencies (18, 38, 70, 120 and 200 kHz). These multifrequency TS data will assist with acoustic identification and biomass estimation of lanternfish that, in turn, will enable contribution of much-needed lanternfish data to ecosystem models.

Keywords: Target strength, acoustic, swimbladder, Prolate Spheroid Model, Distorted Wave Born Approximation Model, lanternfish, mesopelagic fish, Northeast Atlantic, myctophid, *Benthosema glaciale, Notoscopelus kroeyerii, Myctophum punctatum*.

ACKNOWLEDGEMENTS

I am highly grateful to my supervisor, Professor Andrew Brierley at University of St Andrews, for his advice and long lasting support.

I thank the cruise leaders (Kristjan Kristinsson and Hjalmar Vilhjalmsson), Captain, crew and researchers on board the research vessel Arni Fridriksson, Marine Research Institute (MRI) in Iceland, for help and support. Thanks to Thorsteinn Sigurdsson and Hedinn Valdimarsson at MRI for granting access to data and for practical advice, Hrafnkell Eiriksson at Marel in Iceland for radiographic advice at an early stage of the project, and to Maria Kotlyar at the University of St. Andrews for translation of Russian literature.

I am in grate gratitude to Dr. Hiroki Yasuma, Dr. Yoshimi Takao and Dr. Kouichi Sawada for making the radiographic measurements possible by inviting me to their laboratory in Japan and further I thank them for their help and advice on target strength models and for their amazing hospitality during my stay in Japan.

Also thanks to other staff and scientists at National Research Institute of Fisheries Engineering, Ibaraki, Japan for great hospitality and support during my visit to work at the Institute's laboratory. This study was partly supported by a grant from Marine Research Institue in Iceland.

Further, I would like to thank the examiners: Professor Anne Magurran and Dr. Dezhang Chu for their comments and suggestions that truly added more value to my work.

I am endlessly grateful to my family, Guðlaug Björnsdóttir, Bárður Örn Birkisson, Björn Hólm Birkissson and Freyja Birkisdóttir for all the support and understanding.

MOTIVATION

In June and July 2001 I was on board the Icelandic research ship Bjarni Sæmundsson participating in a joint international multi-ship trawl and acoustic survey on pelagic redfish (*Sebastes mentella*) in the Irminger sea and adjacent waters (Anon. 2002). My responsibility was to coordinate biological sampling on board the vessel as well as observe potential redfish acoustic signals from the echosounders in collaboration with Páll Reynisson, the cruise leader. During this off shore cruise I observed the continuous deep scattering layers (DSL) at several hundred meters depths (Magnusson 1996; Sigurdsson *et al.* 2002) and was informed that this was most likely due to mesopelagic fish dominated by lanternfish (Family: Myctophidae) and also zooplankton, while our midwater trawls designed for catching redfish were not suitable to catch the small myctophid fish. Good portion of the DSL moved to shallower depths at night indicating extensive diurnal migration. This inspired my curiosity and interest for the biology of myctophids and the function of the mesopelagic ecosystem. Hence, I went with high excitement on my next cruse into Irminger sea (Anon. 2003) in summer 2003 but this time we also had a fine meshed trawls and indeed we observed that myctophids were dominating the catches from the DSL. In continuance I was determined to study the biology and ecology of myctophids, but lack of information on myctophids was obvious and quite difficult to get hands on the results from some of the few studies on myctophids (possibly because often myctophid observations were a by product of other research). Also the scarcity of quantitative data was prominent since net sampling was unreliable due to net avoidance and also impractical due to long distances and depths. Further the limited knowledge on the acoustic backscatter of common myctophid species in

Irminger sea was surprising, but acoustics are probably the most immediate approach for quantitative estimates of the myctophids.

This thesis reviews the ecology of dominant myctophid species in Irminger sea and provides multifrequency target strength data that will assist with acoustic identification and biomass estimation of lanternfish that contributes much-needed lanternfish data to ecosystem models.

LIST OF ACRONYMS

TS	target strength
EL	echo level
TL	transmission loss
SL	source level
RSM	resonance prolate spheroid backscattering model (Love 1978; Ye 1997a)
PSVM	prolate spheroid void (exact soulution) model (Furusawa 1988)
ESM	exact solution spherical backscattering model (Anderson 1950)
DWBA	distorted wave Born approximation backscattering model (Chu *et al.* 1993; Stanton *et al.* 1993; Lavery *et al.* 2002)
DSL	deep scattering layer
CZCS	coastal zone colour scanner
SL	standard length
m	metre
mm	millimetre
cm	centimetre

1 GENERAL INTRODUCTION

1.1 The abundant lanternfish in the north east Atlantic

In the north east Atlantic, lanternfish or myctophids (Family: Myctophidae) are an important component of the geographically extensive sound scattering layers at depths down to 800 m (Farquhar 1977; Gjosaeter & Kawaguchi 1980; Magnusson 1996; Sigurdsson *et al.* 2002; Anderson *et al.* 2005). The combined biomass of myctophids and other mesopelagic fish in these layers is believed to be very high, but has only been evaluated roughly because of limited data: Gjosaeter & Kawaguchi (1980) estimated the total mesopelagic fish biomass to be 14.47 million tonnes in the north east Atlantic, mainly based on catches in micronekton nets and partly by echo integration. Further, many myctophid species undergo extensive diurnal vertical migrations ranging up to several hundred meters. The small but abundant myctophid fish are important food source and are likely to have essential function in vertical energy transfer in the mesopelagic ecosystem. Also they are effective zooplankton predators.

However there is general lack of knowledge about basic concepts of the biology and ecology of myctophids because sampling and observation of the off-shore mesopelagic ecosystem is made difficult by several factors, including large horizontal and vertical distances, high pressure at sampling depths, light sensitivity of the target organisms that live in a habitat of near-perpetual darkness, and gear avoidance. Further, the results from myctophid studies can be somewhat hard to get as discussed

in the motivation chapter. Hence I include a literature review on the ecology of the species here studied.

The sampling limitations mentioned above leave underwater acoustics as a very important tool for estimation of abundance and distribution of the oceanic myctophids and other components of the ecosystem (Medwin & Clay 1998; Horne 2000; Simmonds & MacLennan 2005). As described in more detail later in this introduction the target strength is a logarithmic measure of the proportion of the incident energy which is backscattered by the target. Knowledge of the target strength of the individual fish targets that are contributing to the received acoustic signal is essential for calculation of numerical abundance and biomass estimates (Simmonds & MacLennan 2005). There is, however, a general lack of information on the backscattering properties of myctophids and other mesopelagic fish in the northeast Atlantic.

Ecosystem models can e.g. be used to describe some functionality through the ecosystem i.e. carbon flow from primary production to top predators and for an instance indicate the functionality of important species or trophic groups. Recent studies have shown importance of mesopelagic fish (mainly myctophids) in active (fish mediated) transport of carbon out of the epipelagic zone (Davison *et al.* 2013) in a such scale that it should be applied to models of the global carbon cycle. Further, recent large scale acoustic estimates of mesopelagic fish biomass (Kloser *et al.* 2009; Irigoien *et al.* 2014) suggest significantly more biomass than earlier, net sampling, predictions. Although this has for long time been suspected (e.g. Gjosaeter & Kawaguchi 1980) and net avoidance been documented (Heino *et al.*; Kaartvedt *et al.* 2012), better understanding of the acoustic properties of mesopelagic fish, including myctophids, needs to be documented before this can be properly evaluated.

In this study I will predict the acoustic backscatter of three abundant myctophid species in the north east Atlantic using theoretical models. The results give the first length related target strengths for those species at several acoustic frequencies that will importantly contribute to much-needed quantitative estimates of myctophid abundance.

1.2 Ecology of myctophid fish in the Northeast Atlantic (literature review)

1.2.1 *Introduction*

In the North-East Atlantic (Figure 1), extensive deep acoustic scattering layers of varying intensities have been observed by echosounders throughout vast areas at depths between 0 and 800 m (Farquhar 1977; Gjosaeter & Kawaguchi 1980; Magnusson 1996; Sigurdsson *et al.* 2002; Anderson *et al.* 2005). A great variety of pelagic organisms are found in these layers, but the major components are believed to be myctophid fish (Myctophidae), Gonostomatidae, Stomiidae, jellyfish, cephalopods and euphausiids (Kawaguchi & Mauchline 1987; Magnusson 1996). The combined biomass of these organisms is believed to be very high, but has only been evaluated roughly (Gjosaeter & Kawaguchi 1980).

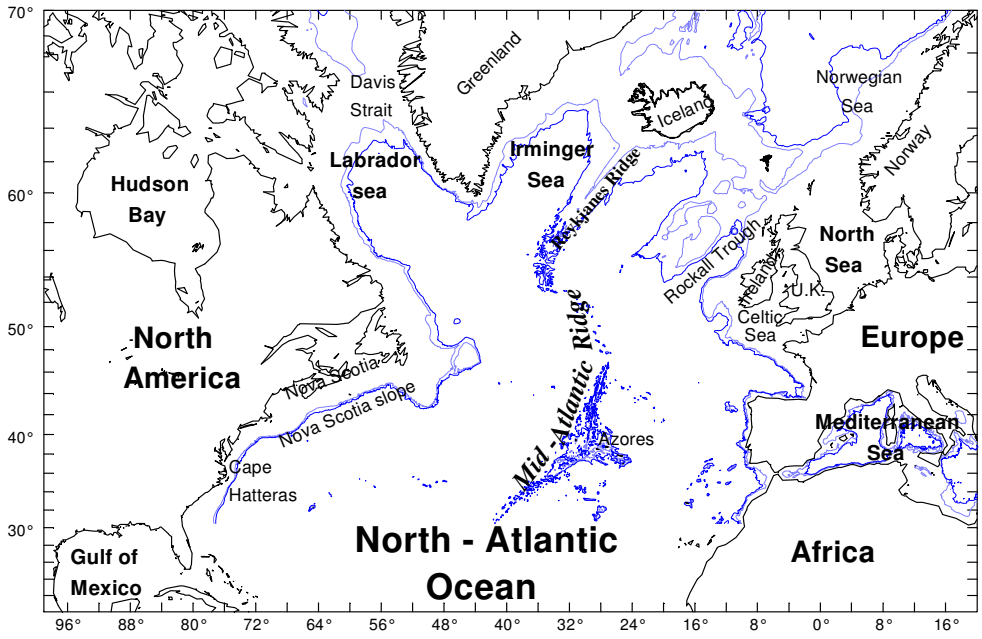

Figure 1 The North-Atlantic Ocean. = 1000 m depth, = 2000 m depth.

Stocks of the commercially important pelagic redfish (*Sebastes mentella*) in the Irminger Sea and adjacent waters have been estimated to have biomass of more than 2 million tonnes (Anon. 2002). This species interacts with the deep scattering layers, feeding mainly on zooplankton but also occasionally on myctophids (Magnusson & Magnusson 1995). There is increasing interest in the fish species that make up the deep scattering layers of the open ocean. Myctophids have been found in considerable abundances at mesopelagic depths (200-1000 m) in most areas of the worlds oceans, and hence apparently make an important link in the mesopelagic food web. Further, diel vertical migrations of myctophids are subject to considerable active vertical transport of organic matter.

This section reviews current knowlegde on three chosen myctophids having subpolar-temperate distribution (Figure 2) in the Atlantic Ocean as described by

Backus et. al. (1977). The species are: *Benthosema glaciale*, *Notoscopelus elongatus* and *Myctophum punctatum* and have been chosen here because they are belived to have ecological importance in the subpolar-temperate area and their biology has been studied considerably at least compared to many other mesopelagic fish species. Amongst these *B. glaciale* has been by far the most studied.

1.2.2 *Zoogeography*

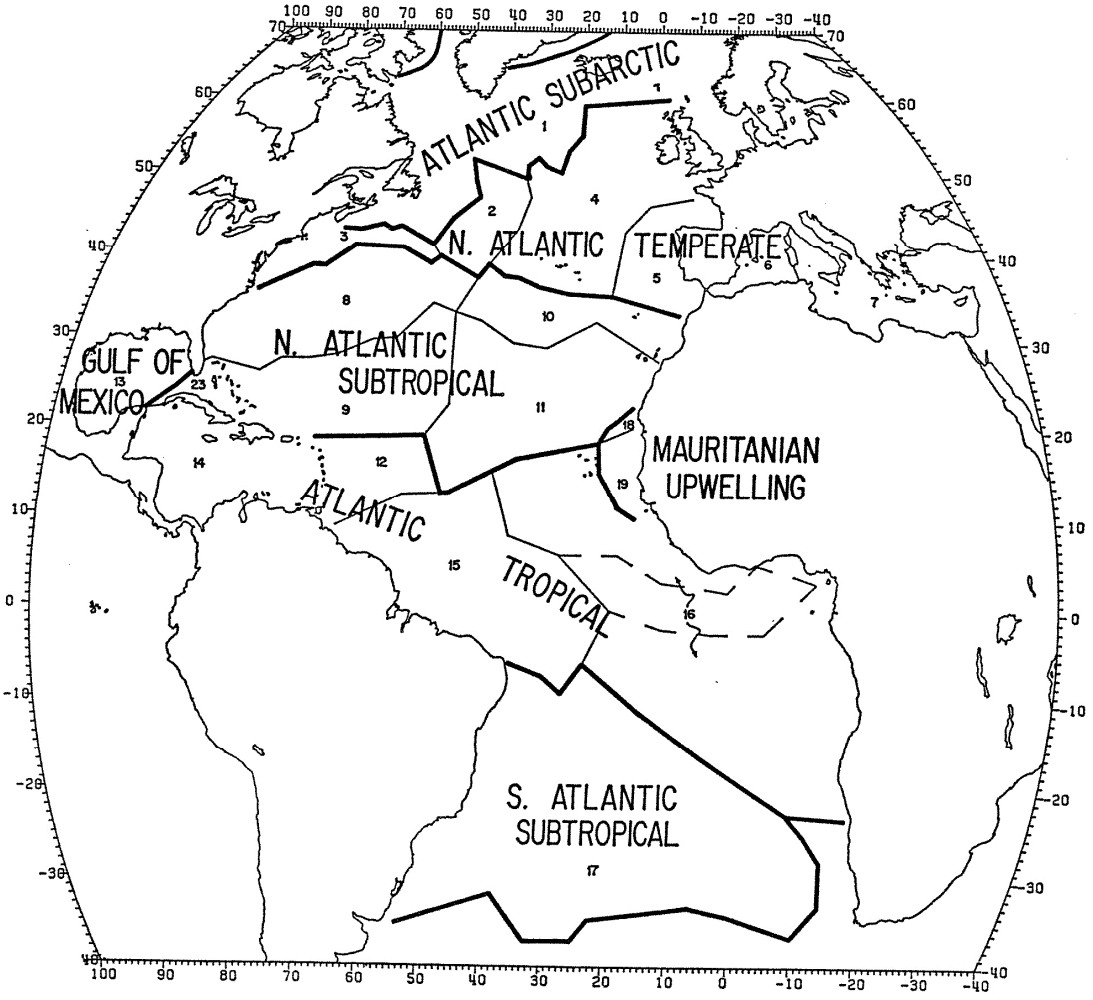

Figure 2 Atlantic faunal regions and provinces. Heavy lines separate regions, light lines provinces (Backus *et al.* 1977).

Backus et al. (1977) described faunal regions and provinces of the Atlantic Ocean (Figure 2) using extensive myctophid samples. Although based on the distribution of

myctophids, they reasoned it to be generally applicable to pelagic organisms. The comparative atlas of zooplankton (van der Spoel & Heyman 1983) reveals extensive selection of distribution maps dealing with pelagic biogeography. In this atlas the diversity of distribution patterns shows that pelagic biogeographical maps can hardly be established from distribution patterns of single group of species. Longhurst (1995; 1998) determined four primary biomes, subdivided into several provinces (Figure 3). He used pelagic production patterns, mainly based on chlorophyll distribution, estimated from satellite Coastal Zone Colour Scanner (CZCS). On a monthly basis, abundance and rate of change of plankton communities were described globally. For the foreseeable feature this might be the most precise and practical method in predicting the pelagic biogeography.

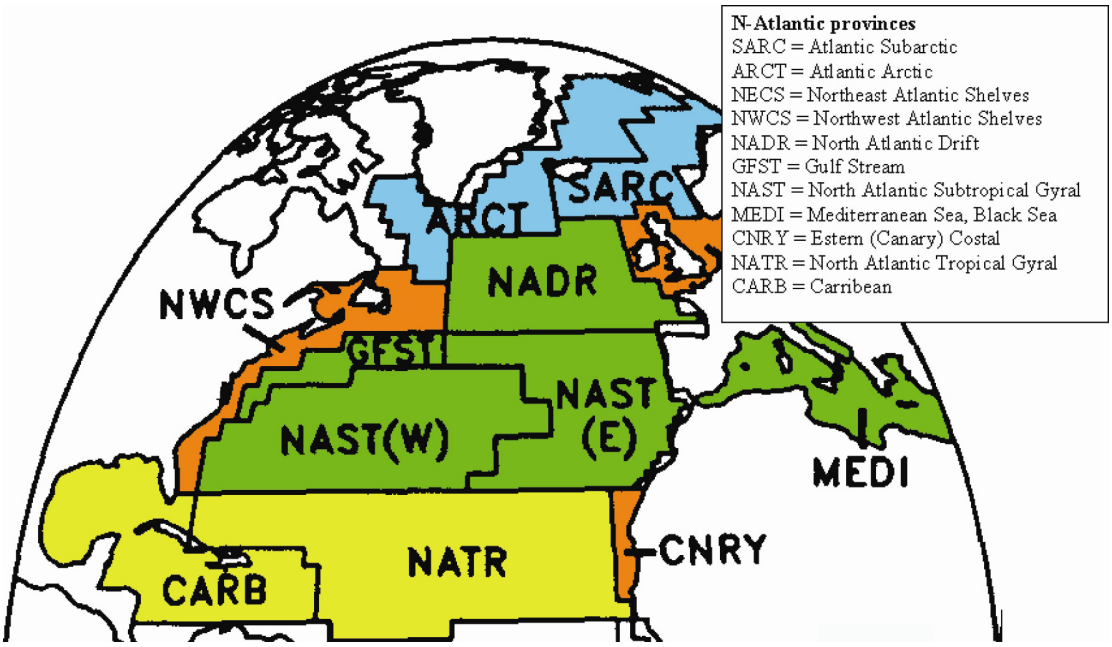

Figure 3 Map of biogeographic biomes and provinces.

Biomes: Atlantic Polar, Atlantic Costal, Atlantic Westerly Winds, Atlantic Trade Wind. (Modified from Longhurst (1998)).

Some dissimilarities between the province maps of Longhurst and Backus et. al. suggest that the latter to be considered mainly as distributional system that describes faunal clusters of myctophid fish associated with coherent physical zones of the ocean. Current systems and water circulation are important factors in structuring the zoogeography of the pelagic ecosystems (Anderson *et al.* 2005). Backus and Craddock (1977) have also demonstrated that the faunal provinces can also be viewed as sound-scattering provinces.

1.2.3 *Mesopelagic fish abundance*

Mesopelagic fish abundance estimates were reviewed for the Northeast Atlantic by Gjosaeter and Kawaguchi (1980) on the basis mainly of micronektonic trawl and acoustic data.

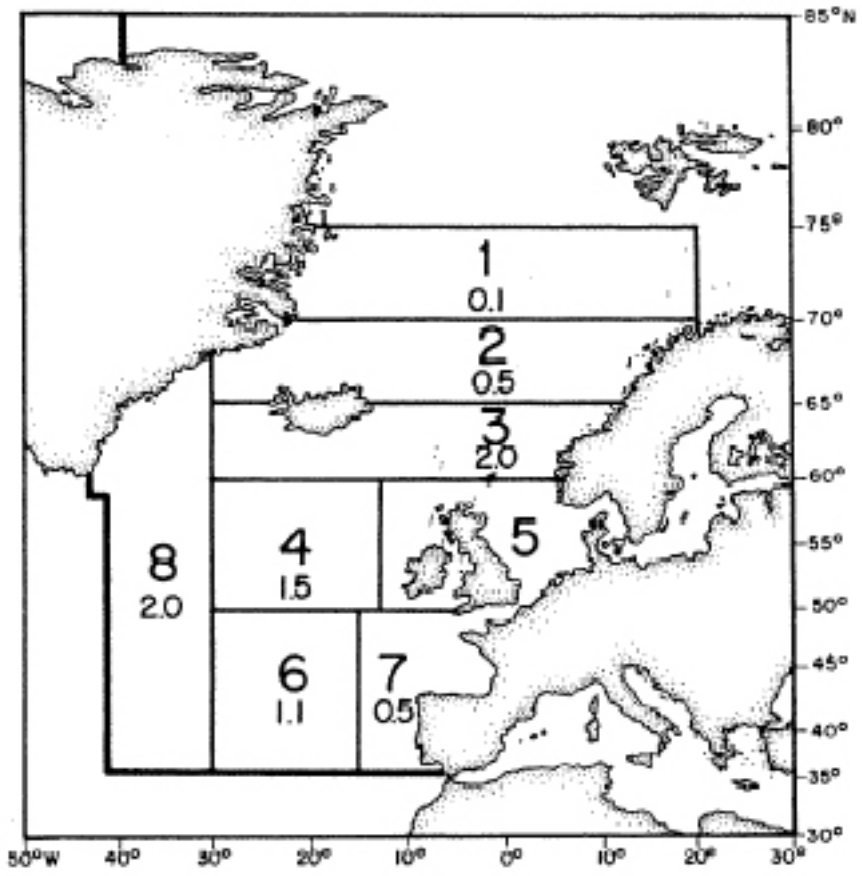

Figure 4 Mean mesopelagic fish biomass in g/m2 (smaller figures) in eight regions (large figures) of the Northeast Atlantic (Gjosaeter & Kawaguchi 1980).

They divided the northeast Atlantic into 8 sub-areas and estimated the mean biomass to be between 0.1 and 2.0 g/m^2 (Figure 4) and stated that the fish families Myctophidae, Gonostomatidae and Sternoptychidae totally dominate the mesopelagic fish fauna in the area. The total mesopelagic fish biomass was estimated to be 14.47 million tonnes. They found highest concentrations of mesopelagic fish in the neritic areas off southern Norway and west of the British Isles and estimated mean biomass in these areas to be at least of the order of 10 g/m^2, but also noted that it was not known if similar concentrations were near Iceland and southern Greenland. Most of those abundance numbers were believed to be underestimates.

1.2.4 *Biology of Myctophid fishes*

Larvae of Myctophidae species show high morphological diversity (Sabates & Saiz 2000). The shape of their body can vary from slender to robust. There are e.g. inter-specific differences in the larvae eye morphology and size, and some genera have eyestalks (Figure 5).

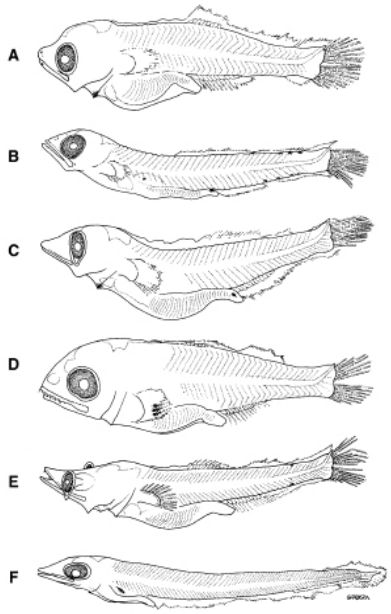

Figure 5 Myctophiform larve collected from the Catalan Sea. (A) *Benthosema glaciale* 6.16 mm, (B) *Ceratoscopelus maderensis* 6.36 mm, (C) *Hygophum benoiti* 6.48 mm, (D) *Lampanyctus crocodilus* 6.48 mm, (E) *Myctophum punctatum* 8.16 mm, (F) *Notolepis rissoi* 13.02 mm (Sabates & Saiz 2000).

The family Mictophidae is divided into the sub-families Myctophinae (larvae with elliptical eyes) and Lampanyctinae (larvae with rounded eyes) (Sabates & Saiz 2000). These differences in eye morphology may have an adaptive role related to the vertical position of the larvae in the water column. In the Mediterranean larvae of Lampanyctinae species have been found mainly in the upper 30 m (Olivar & Sabates

1997) while larvae of Myctophinae have a deeper distribution, generally 25-75 m (Olivar *et al.* 1998; Sabates & Saiz 2000). In the Mediterranean it has also been observed that high morphological diversity between larvae of Myctophid species results in considerable variability in their diet and feeding strategies. This morphological diversity was suggested to be a possible adaptive factor leading to optimized utilization of the oligo-trophic open-ocean habitat (Sabates & Saiz 2000).

Most myctophids have diel vertical migration, often for several hundred meters, but it has been shown that not all individuals of any particular, vertically migrating population move up every night. Much less extensive migration has been observed among some deeper-dwelling myctophid species. In general juveniles occupy shallower reaches of the depth range of any given species (Nafpaktitis *et al.* 1977) .

1.2.4.1 Benthosema glaciale

Benthosema glaciale (Figure 6) is considered the dominant mesopelagic fish species in most of the northeast Atlantic (Nafpaktitis *et al.* 1977; Gjosaeter & Kawaguchi 1980).

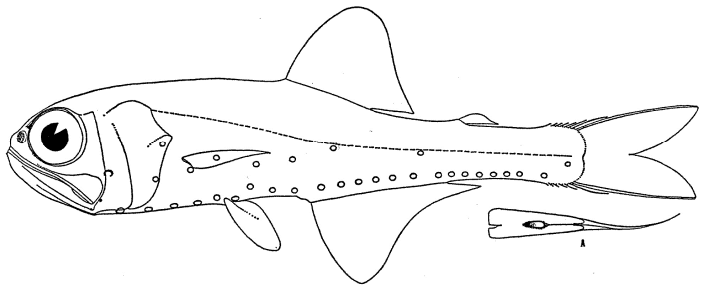

Figure 6 *Benthosema glaciale*: young female, 54mm; A, supracaudal gland of male, 64mm (Nafpaktitis *et al.* 1977).

Compared to other myctophids, its biology has been much studied in several areas of the North Atlantic and adjacent waters e.g. (Halliday 1970; Gjosaeter 1973b;

1973a; Kinzer 1977; Gjosaeter 1978; Badcock 1981; Gjosaeter 1981a; Kawaguchi & Mauchline 1982; Kinzer 1982; Roe & Badcock 1984; Sameoto 1988; Sameoto 1989; Dalpadado *et al.* 1998; Sabates & Saiz 2000; Acevedo & Fives 2001; Suneetha & Salvanes 2001; Sabates *et al.* 2003a; Sabates *et al.* 2003b; Fock *et al.* 2004; Sabates 2004).

1.2.4.1.1 Distribution

Benthosema glaciale is a subpolar-temperate species (Figure 7).

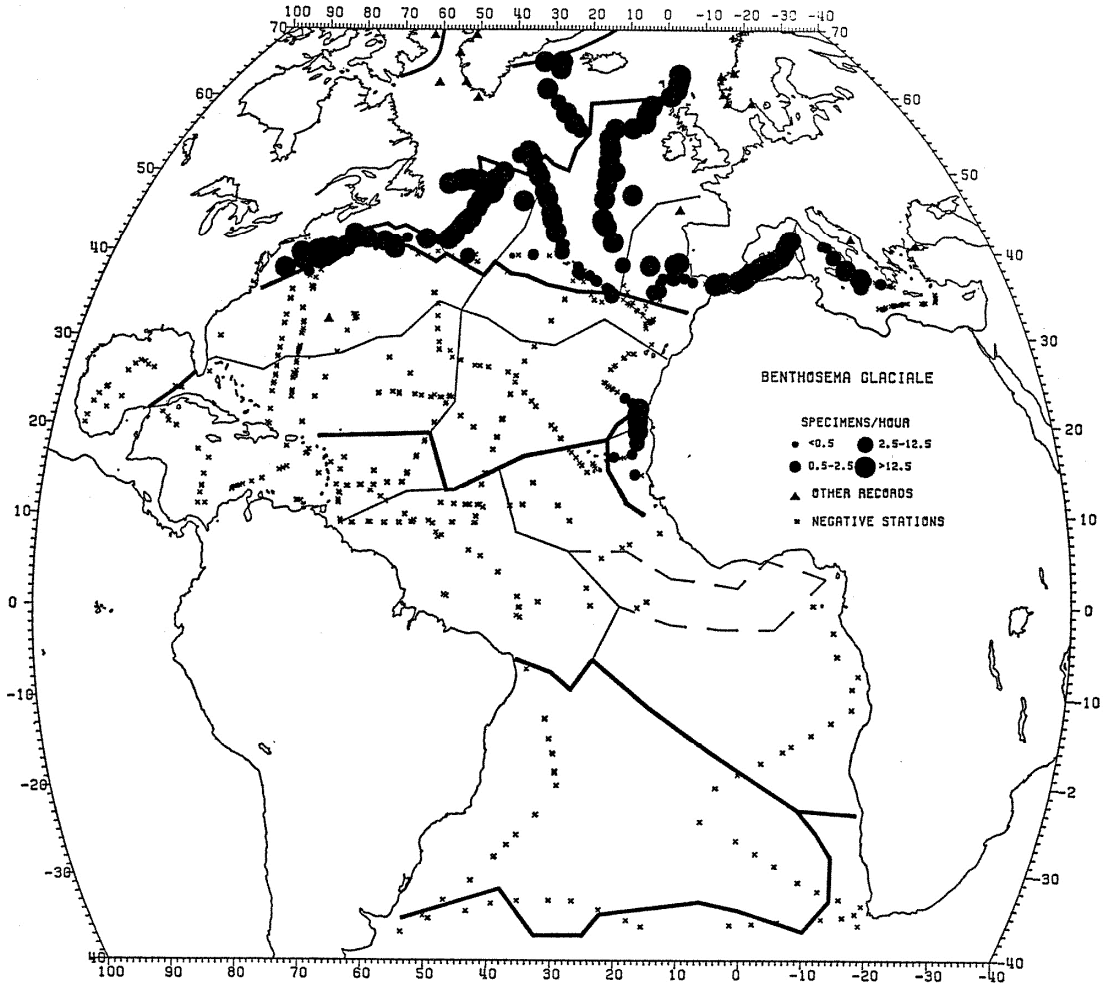

Figure 7 Distribution of *Benthosema glaciale* as presented by Nafpaktitis et al. (1977).

B. glaciale has been observed as the most important myctophid in most of the subArctic and temperate areas of the North Atlantic and extends its distribution in to the Mediterranean. The northerly distribution of *B. glaciale* reaches to Greenland (Western N-Atlantic) and to Spitzbergen (Eastern N-Atlantic). Its southerly boundaries are believed to be from Cape Hatteras in the West, to the Mauritanian upwelling area west off Africa in the East Atlantic (Nafpaktitis *et al.* 1977).

1.2.4.1.2 larvae

Kawaguchi and Mauchline (1982) concluded that *B. glaciale* larvae are present in the Rockall Trough from April to September, but principally in the first half of this period. They grouped the developmental stages as following:

I. Before notochord flexion (3.2 – 6.5 mm)

II. Notochord in process of flexion, lower caudal lobe not developed. (5.5-7.6 mm)

III. Notochord flexion completed; lower caudal lobe developed with its posterior tip slightly behind or below upper lobe; usually the dorsal fin anlage clearly recognizable. (6.5-10.5 mm).

IV. Metamorphosis (transitional) stage; anal photophores recognizable.

They found *B. Glaciale* larvae at developmental stage I only at depths above 75 m, but stage II larvae were found at depths deeper than 100 m. Ropke (1989) gives the depth-range for *B. glaciale* larvae as 40 – 110 m. Metamorphosing larvae have been observed below 500 m both in the Atlantic and Mediterranean (Tåning 1918). This suggests that at notochord flexion stage the larvae begin to sink below 100 m depth and that metamorphosis takes place below 500 m. During metamorphosis there is no increase in standard length. Kawaguchi and Mauchline (1982) concluded that metamorphosis completes in a very short period of time compared with other

developmental stages and that it occurred mainly in the period June-July, but also possibly in August . In the Mediterranean *B. glaciale* larvae have been observed feeding mainly on copepod eggs and nauplii, while post-flexion larvae consumed calanoid copepodites. That study also showed a clear relationship between feeding pattern and light intensity (Sabates *et al.* 2003a).

1.2.4.1.3 Juvenile and adult growth

Seasonal size frequency distribution of *B. glaciale* juveniles and adults in the Rockall Trough show detectable modes of size ranges for zero- and one-year-old fish, and maybe two year old fish, but further modes are difficult to distinguish, possibly owing in part to low density and net avoidance of this size group.

The new juvenile zero group recruitment was observed in July just after larvae metamorphosis. These juveniles had size range of 10-19 mm. Wide size modes reflect long spawning season of *B. glaciale* in the Rockall Trough and hence overlapping size ranges of different age groups (Kawaguchi & Mauchline 1982). This overlapp was also observed in the north-western Atlantic (Halliday 1970) and off Norway (Gjosaeter 1978). Seasonal growth rate (Figure 8) is higher during the summer particularly for younger year-classes.

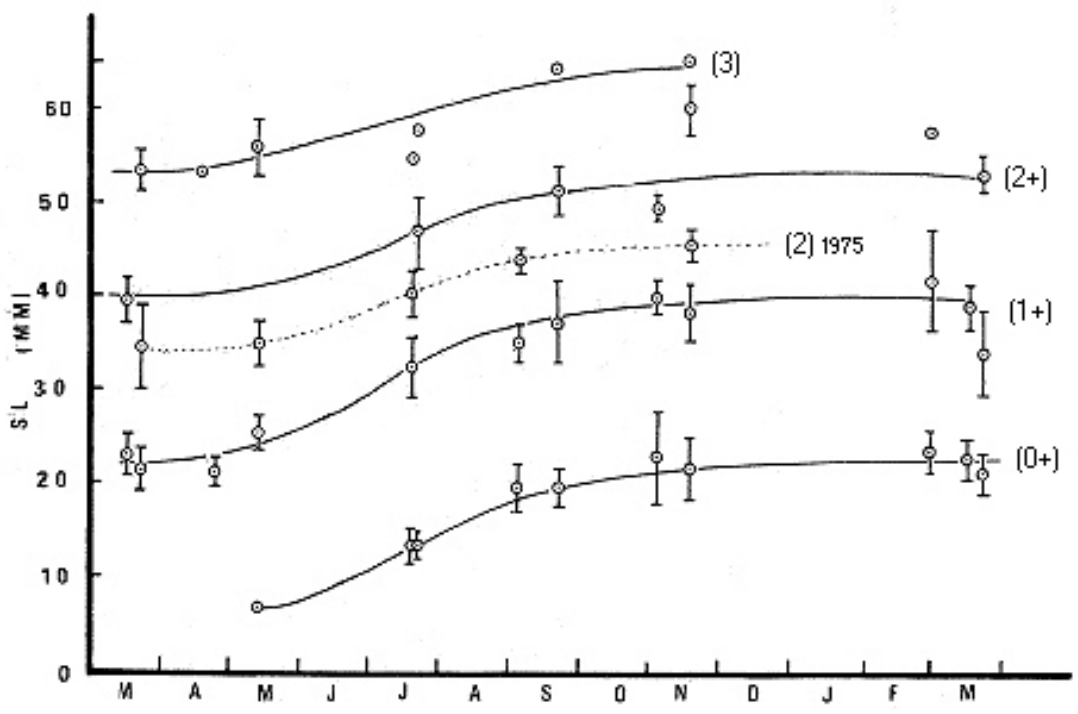

Figure 8 Growth curves of *Benthosema glaciale* in the Rockall Trough, based on average standard lengths of modes in different months. Estimated year classes in parentheses. Vertical lines indicate +/- 1 standard deviation. Broken line showes curve for 2 year old fish in 1975 (Kawaguchi & Mauchline 1982).

Increments of length in the first and second year were estimated as 18 and 13.5 mm respectively in the Rockall Trough (Kawaguchi & Mauchline 1982), and were similar to values of 19.5 and 12.8 mm from western Norway (Gjosaeter 1981a). Kawaguchi and Mauchline (1982) concluded that growth rates of *B. glaciale* in the Rockall Trough and Norwegian waters observed by Gjosaeter (Gjosaeter 1973a) were higher than in north-western Atlantic populations observed by Halliday (1970). However, in the Nova Scotia Slope area Sameoto (1988) found considerably larger specimens (83 mm maximum size) than Halliday (1970) had observed (58 mm max. size). Sameoto suggested that the Isaccs-Kidd midwater trawl used by Halliday might be less efficient at capturing larger *B. glaciale* than the BIONESS multiple net sampler used by Sameoto. In the Rockall Trough there were indications of annual

variability in growth rate, in this case resulting in smaller 2 year class in year 1975 than observed in other years. Possible causes of the growth variability were not discussed by the authors (Kawaguchi & Mauchline 1982).

1.2.4.1.4 Gonad development and reproduction

In the Rockall Trough mature ovaries were found to be filled with easily separable eggs, over 0.3 mm in diameter, just prior to spawning. Immature ovaries contained smaller eggs more difficult to discern with naked eye (Kawaguchi & Mauchline 1982). Sex can be distinguished externally from the infracaudal and supracaudal luminous plates (sexual dimorphism), which begin to appear at a body length of 25 mm. Males have small, undivided supracaudal luminous gland framed by black tissue. Females usually have 2 very small, roundish patches of infracaudal luminous tissue. Occasionally individuals may have both supracaudal and infracaudal glands, but then the supracaudal is better developed in males and the infracaudal in females (Nafpaktitis *et al.* 1977). In the Rockall Trough in year 1975 spawning had not taken place in the latter part of March, but at that time female gonads were observed in a state just prior to spawning. This indicates that in this area spawning starts in April-May (Kawaguchi & Mauchline 1982). In the Celtic Sea and West Coast of Ireland in 1998 *B. glaciale* spawning was observed mainly at oceanic stations, as presence of yolk-sack larvae (3.5-5 mm) sampled down to 200 m, from March to July (Figure 9).

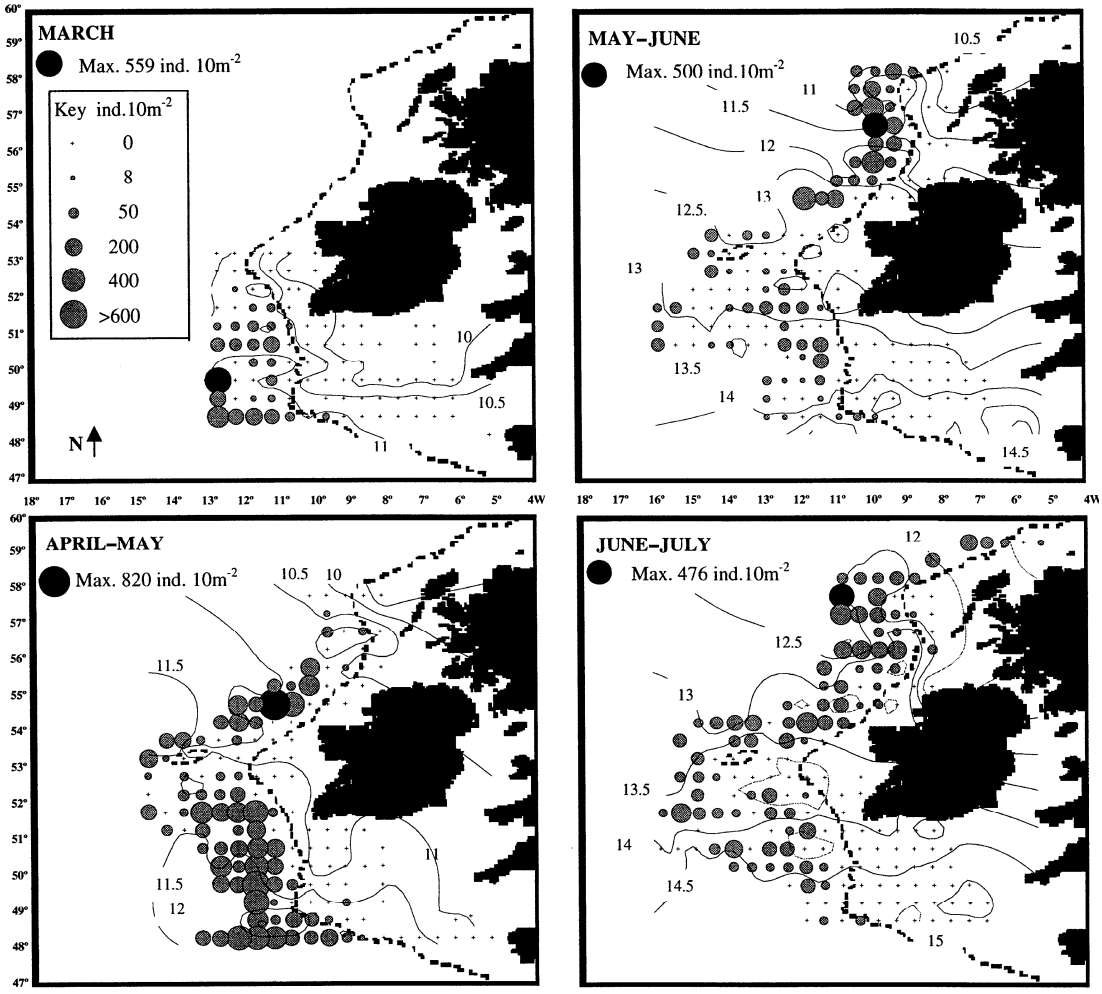

Figure 9 Distribution and abundance of *Benthosema glaciale* larvae over four sampling periods West and North off Ireland (Acevedo & Fives 2001).

The bulk of spawning appeared to take place in spring and a northward shift of the maximum larval abundances was noted with majority of larvae recorded at water temperatures between 11-12.5°C (Acevedo & Fives 2001). This time of spawning is in accordance with observations off Nova Scotia, where ripening *B. glaciale* were caught in January and February and larvae occurred in May and July (Halliday 1970).

Breeding was found to be size dependent in the Rockall Trough. During the breeding season all individuals at size range less than 30 mm sL were immature; only a portion of the 2 year old fish in the size range of 30-39 mm were mature, and all 2

and 3 year old fish larger than 40 mm bred during the breeding season in the Rockall Trough (Kawaguchi & Mauchline 1982).

Off Nova Scotia Halliday (1970) also found that part of the *B. glaciale* population spawns 2 years old (37.5 mm mean sL) and all 3 years old (46.3 mm mean sL) and subsequent ages were spawning.

Fecundity has been found to increase with size in the Rockall Trough (Kawaguchi & Mauchline 1982) and in Norwegian waters (Gjosaeter 1981a). In the Rockall Trough *B. glaciale* females produced 133 – 624 eggs (Kawaguchi & Mauchline 1982). The average percentage of females in samples was 53% and 55% in the Rockall Trough (Kawaguchi & Mauchline 1982) and Norwegian waters (Gjosaeter 1973a) respectively, with one exception: in March 1975, in the Rockall Trough, females comprised 69% of the adult fish. This uneven distribution might indicate schooling behaviour just before the breeding season (Kawaguchi & Mauchline 1982).

1.2.4.1.5 Feeding

1.2.4.1.5.1 Time of feeding and feeding behaviour

B. glaciale has in general been found to feed primarily at night. Feeding usually continues during the day but at a reduced rate e.g. (Kinzer 1977; Sameoto 1988).

In the upwelling area at slope waters of NW Africa, Kinzer (1977) observed diel migration of *B. glaciale,* from 150-400 m day-time depths, to near surface night-time depths (25-100 m). Kinzer (1977) suggested that the small range of vertical migration was caused by reduced light as consequence of high primary production in this

upwelling area. Further, he found evidence for intensive nocturnal feeding of *B. glaciale* mostly occurring in the evening or early night.

In the spring at the Nova Scotia Slope the entire *B. glaciale* population migrated into the upper layers at dusk and fed mainly on copepods during the night in the upper 200 m. Some daytime feeding was though observed at depths greater than 300 m (Sameoto 1988). In the Davis Strait *B. glaciale* was concentrated at 300 – 500 m during the day (individuals found down to 900 m), in the upper part of the Labrador Sea water mass (3,5° – 4 °C). At night 46% of the *B. glaciale* population was found in the upper 60 m, but no *B. glaciale* individuals were found at the cold water 65 – 150 m depth interval. The remaining 54% of the population spent the night at 150 – 550 m (Sameoto 1989).

During the night in the Nova Scotia Slope, the majority of the population was found below the main concentration of copepods which was in the upper 30m. Suggesting that most fish feed below the highest concentrations of prey or else make short excursions into the upper layers to feed and then return to the deeper water. The latter possibility is further supported by high percentage of *Calanus* (concentrated in 30-50 m) in stomachs of fish in the top 200 m (Sameoto 1988). Sameoto (1988) further suggested that the few *B. glaciale* caught in the upper 30 m during the day were forced by hunger from the normal diurnal migration, based on their empty stomachs. In Davis Strait Sameoto (1989) also found that *B. glaciale* in the upper 65 m concentrated 30 – 40 m below the main concentration of copepods at 10 – 20 m. Hence, at night the majority of fish were at depths having copepods concentrations of 200 – 380 m^{-3}, but no myctophids were found in the top 10 m where copepod concentration was as high as 939 m^{-3}.

1.2.4.1.5.2 Prey composition and selectivity

In the Rockall Trough more than 90% of the items eaten by *B. glaciale* (9.2-62.5 mm sL) were copepods and 81.1% of the fish with food present in their stomachs had fed exclusively on copepods (Kawaguchi & Mauchline 1982). Other organisms found were of minor dietary importance. *Pleuromamma* copepods were most frequently eaten, mostly *P. robusta*. Each full stomach contained the average number of 2.6 prey organisms. Ontogenetic changes in the diet were apparent. Major diet component of the smallest fish were *Calanus* species, mainly *C. helgolandicus*, along with early copepodite stages and other unidentified calanoida. The large calanoid *Euchaeta norvegica*, euphausiids, decapod larvae, and fish only occurred in the stomachs of the larger fish (Kawaguchi & Mauchline 1982).

Feeding of *Benthosema glaciale* in two fjords in Western Norway was studied by Gjosaeter (1973b), who found copepods to be the most common food item in all age groups during all seasons. Euphausiids were common prey items during autumn and winter, but scarce in spring and absent during summer. The majority of one-year and older *B. glaciale* had taken only copepods, but 12% of individuals having recognizable stomach contents had only euphausiids, and 5% had both groups. Partial species determination of the food showed that large copepod species seemed to be preferred, e.g. *Calanus finmarchicus, Metridia sp.* and *Paureuchaeta norvegica*. Stomach contents of 17-20 mm (0-group) *B. glaciale* in October and November showed that they had taken relatively more copepods than older fish, and that smaller copepod species seemed to be preferred.

At the Nova Scotia Slope *Benthosema glaciale* showed highest positive selection for *Pleuromamma* spp., with *P. borealis* as being most common. The much more numerous *Metridia* and *Calanus* species were negatively selected, but calanoid

stage was not identified – hence selectivity index can be misleading, not showing possible selectivity for specific stages. *Pleuromamma* is subject to continuous predation from *B. glaciale* because both species are concentrated at same depths both day and night, on the other hand *Metridia* and *Calanus* were not concentrated at the same night-time depths as *B. glaciale* (Sameoto 1988). In that study *B. glaciale* appeared to broaden its food spectrum with increasing fish length, resulting in wider prey size range and more prey diversity in larger specimens, but there was no indication of increased feeding on euphausiids with increased body length.

In the Davis Strait *B. glaciale* selected *Calanus finmarchicus* stage V and *Calanus hyperboreus* stage IV over smaller stages of these species. Negative selection was on the less abundant *Calanus glacialis* stages IV and V. Species less than 1.5 mm were generally ignored by *B. glaciale*. *Metridia* spp. was consumed in proportion to its numbers in upper strata (15-35 m), but was negatively selected at more depths, possibly because of visual effects (Sameoto 1989).

In upwelling area of NW Africa, copepods (mainly *Pleuromamma* and *Rhincalanus*) and conchoecid ostracods dominated the food of *B. glaciale*, but euphausiids (mostly "adolescent" *Euphausia khronii*) also became a considerable part in night samples (up to 45%) and occasionally amphipods. Only *B. glaciale* longer than 30 mm sL appeared to prefer euphausiids to copepods or ostracods (Kinzer 1977).

1.2.4.2 Notoscopelus elongatus

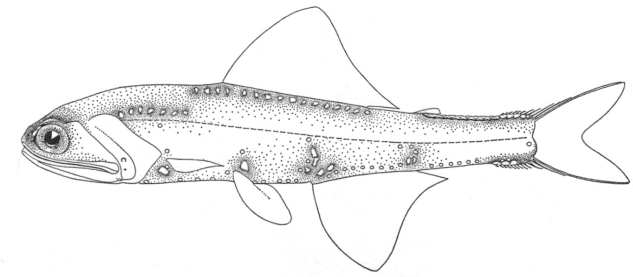

Figure 10 ***Notoscopelus elongatus kroeyeri*****: male, 102.5 mm (Nafpaktitis *et al.* 1977).**

1.2.4.2.1 Distribution

Notoscopelus elongatus (Figure 10) is a subpolar-temperate species that has been divided into two subspecies. *N. elongatus elongatus* in the Mediterranean and *N. elongatus kroeyerii* in the open Atlantic Ocean (Nafpaktitis *et al.* 1977). *N. e. kroeyerii* is found across the North Atlantic Ocean between 40°N and 60°N in the west, and in the east Atlantic between 37°N and the Arctic Circle. *N. e. kroeyerii* is also found in the Mediterranean Sea (Figure 11) (Nafpaktitis *et al.* 1977; Hulley 1984). *Notoscopelus kroeyeri* has been found in considerable abundance off the British Isles, but showing symptoms of population part that has drifted from its suitable habitat, and hence is unable to reproduce (expatriated) (Gjosaeter 1978).

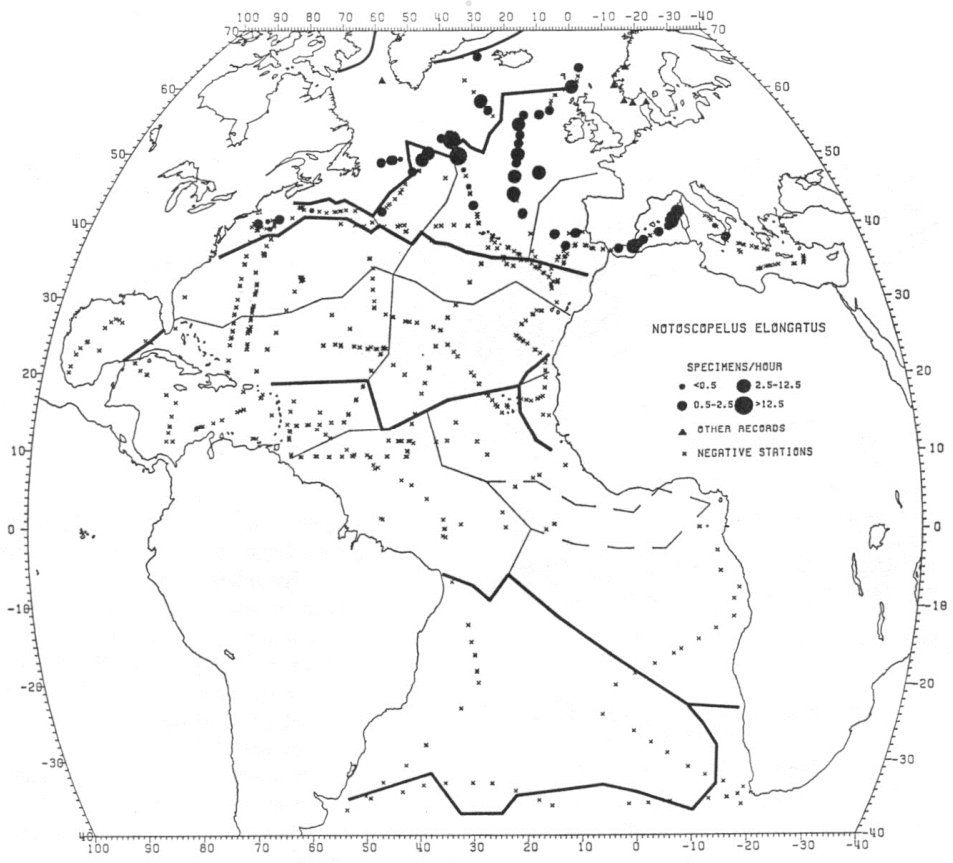

Figure 11 Distribution of *Notoscopelus elongatus* as presented by Nafpaktitis et al. (1977).

N. e. elongatus is known only from the western Mediterranean (Nafpaktitis 1975; Gjosaeter 1981b; Hulley 1984). Nafpaktitis (1975) rationalized the possibility that early stages of *N. e. kroeyerii* are transported by the eastern North Atlantic surface waters flowing into the Mediterranean, where different environmental conditions cause different meristic and morphometric form.

N. elongatus is generally found from the surface to about 150 m during the night, concentrated mainly in the upper 40 m. During the day it is found from 325 m to deeper than 1000 m (Nafpaktitis *et al.* 1977).

1.2.4.2.2 Reproduction

According to Hulley (1984) *N. e. kroeyeri* spawns north and south of the secondary North Atlantic Polar Front. In June east of the Azores Kashkin (1974) found *N. e. kroeyeri* population including juveniles, suggesting that the population was reproducing in the area. In the Rockall Trough Kawaguchi and Mauchline (Kawaguchi & Mauchline 1982) found few adult and larvae individuals and suggested that they were at the northern geographical limit of their breeding populations. Further they concluded that adult *N. e. kroeyeri* occurring further north comprise a true expatriate population. Gjosaeter (1981b) studied population dynamics of *N. e. kroeyeri* west and north of the British Isles and west of Norway in the months December - May. No sign of gonad ripening or of previous spawning, weakly developed luminous glands of the males, and lack of juveniles and larvae, suggested that this was expatriate population maintained by fish drifting from another spawning population. The above mentioned studies did not resolve the questions of the exact time of spawning, or of from which area the *N. e. kroeyeri* individuals drifted from. Common occurrence and wide distribution of adult (8-17 cm total length) *N. e. kroeyeri* as by catch in pelagic redfish trawl (40 mm mesh in codend) in the Irminger Sea (Sigurdsson *et al.* 2002) may suggest that the drift is from population maintained by the anticlockwise circulation of surface waters in the Irminger Sea and/or western Atlantic areas.

1.2.4.2.3 Growth

N. e. kroeyeri has a higher growth rate than the smaller myctophid species that have been studied (Gjosaeter 1981b). Length frequency distributions of *N. e. kroeyeri* from west and north off the British Isles and off the coast of Norway (Figure 12) show

the first age group corresponding well with the first mode in the length frequency distribution while older ages fall into one group. Using a Cassie curve, the second age group was also identified, but the older groups could still not be separated (Gjosaeter 1981b).

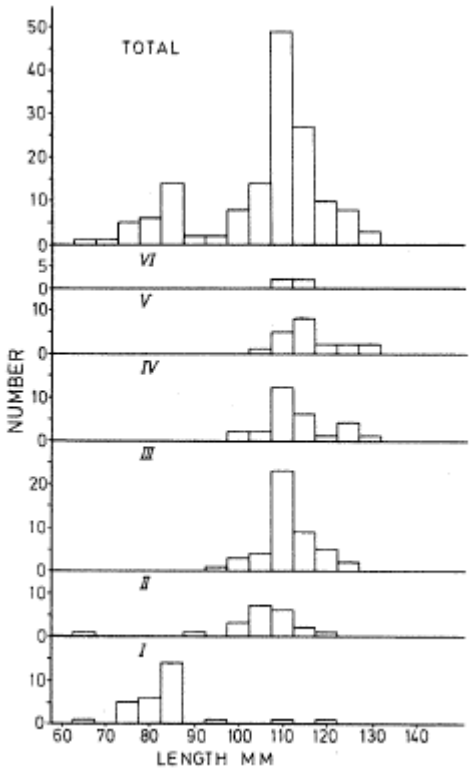

Figure 12 Length distribution of N. e. kroeyeri designed as age group I through VI based on otolith reading (Gjosaeter 1981b).

Growth of *N. e. kroeyeri* sampled from west and north off the British Isles and off the coast of Norway, based on otolith reading, followed the Von Bertalanffy growth curve:

$l_t = 11.91 \text{ cm } (1 - e^{-0.89 (t + 0.17)})$

The length-age relationship can be seen in Figure 13.

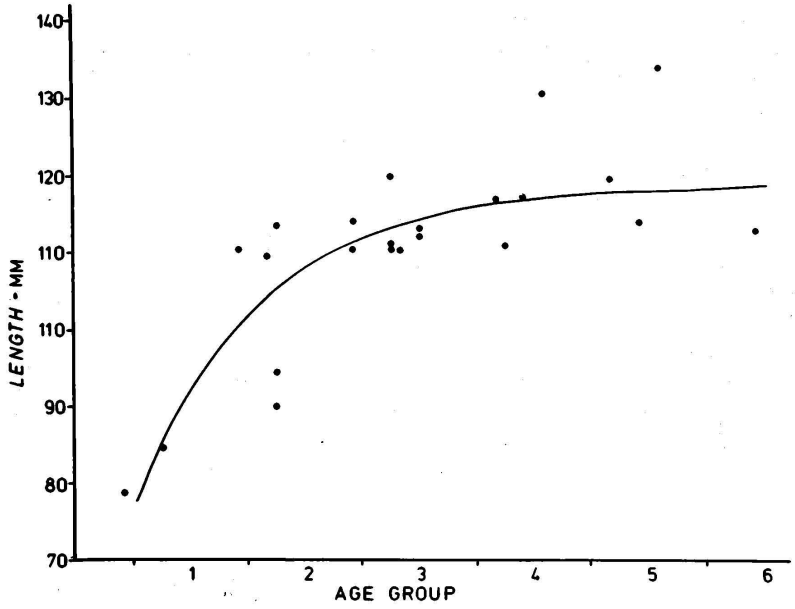

Figure 13 Growth of *N. e. kroeyeri* north and west of British Isles and off the coast of Norway (Gjosaeter 1981b).

In general *N. e. kroeyeri* from Norwegian waters were older than those from west and north of the British Isles, but differences in growth rate were not demonstrated (Gjosaeter 1981b).

1.2.4.2.4 Feeding

Notoscopelus elongatus kroeyeri from west and north off the British Isles and off the coast of Norway mainly feeds on euphausiids. Euphausiids were the only identified prey found in *N. e. kroeyeri* stomachs during winter (December-February). The prey diversity was slightly higher during spring (March-May), when euphausiids remained most important (found in 69% of stomachs), but copepods and other organisms also appeared. In this study feeding seemed to take place at all times, but most intensively at night (03:00-05:00) when nearly 85% of fish had full or extended stomachs. Only 25% or less of fish had this stomach condition at other times. Stomach volume measurements indicated that *N. e. Kroeyery* can eat about 5% of its body weight in one meal (Gjosaeter 1981b).

1.2.4.3 Myctophum punctatum

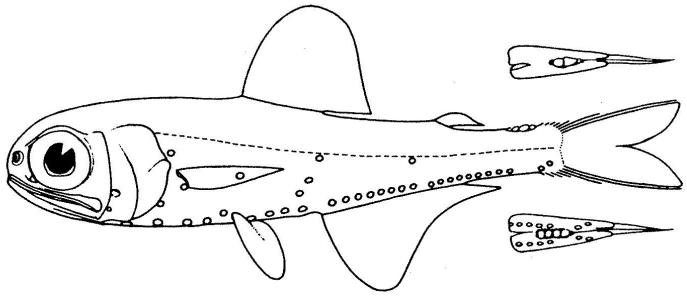

Figure 14 *Myctophum punctatum* (Hulley 1984).

1.2.4.3.1 Distribution

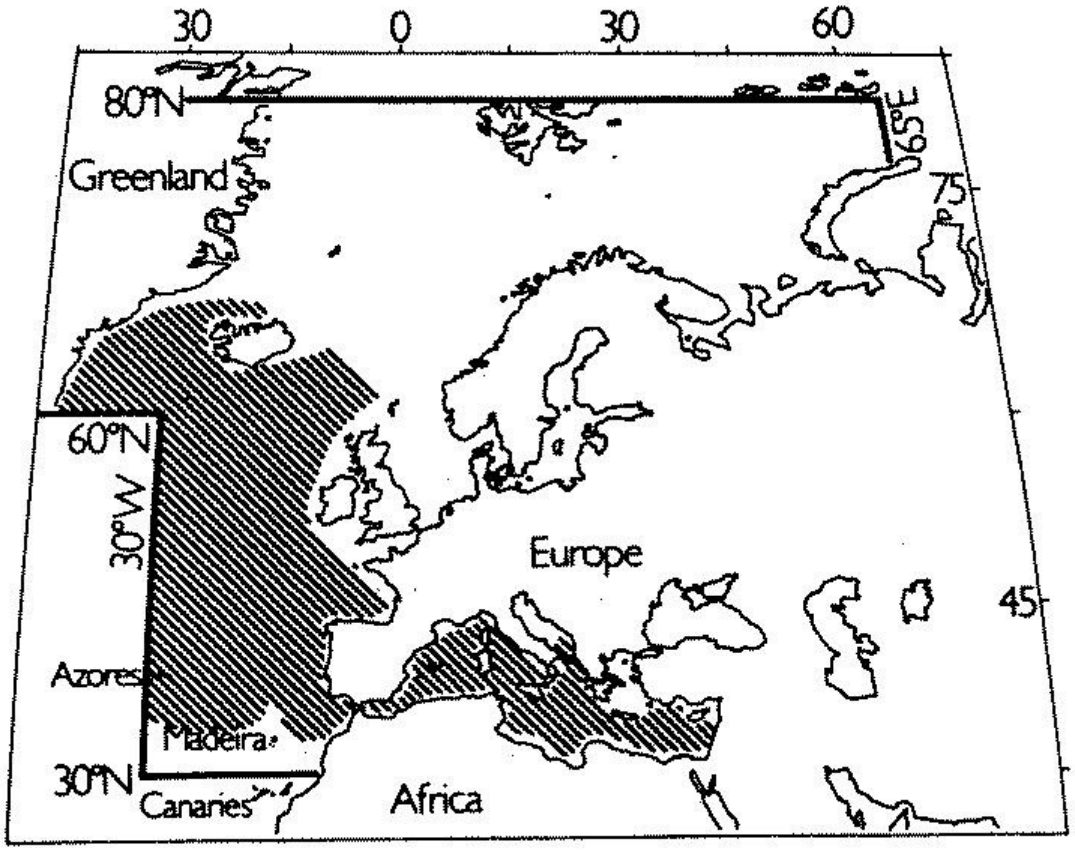

Figure 15 Distribution of *Myctophum punctatum* as described by Hulley (1984).

Myctophum punctatum (Figure 14) is found in subarctic and temperate regions of the North-Atlantic ocean, including the Mediterranean, between 65° and 35° N. Further,

there is seemingly isolated occurrence/stock of *M. punctatum* in the Mauritanian upwelling region, between 20° and 15° N (Hulley 1984). In Irminger sea *M. punctatum* has been recorded to be mainly south of 60° N at depths above and below 500 m (Sigurdsson *et al.* 2002). In the northwest Atlantic, adult *M. punctatum* have been commonly found along continental slopes but seemed unable to reproduce (expatriate) (Zurbrigg & Scott 1972).

M. punctatum has been found from surface down to 1000 m showing diurnal vertical migration toward the surface during the night (Hulley 1984).

1.2.4.3.2 Larvae

The *M. punctatum* larvae belong to the Myctophinae sub-familie and have relatively large jaws and elliptic eyes on eyestalks (Sabates & Saiz 2000). This morphology enables the detection of a greater range of prey in terms of shape and size. Further, *M. punctatum* larvae have retina with high summation ratio and long photoreceptors, indicating a preference for dimmer environments. This could explain observations of increased feeding activity of *M. punctatum* larvae in the Mediterranean at dawn and dusk with less feeding during the brighter daylight hours (Sabates *et al.* 2003a). The *M. punctatum* larvae have rather elongate morphology and notochord flexion occurs at about 7.8 mm sL (Sabates & Saiz 2000).

1.2.4.3.3 Juvenile and adult growth

M. punctatum can reach 107 mm sL and will get sexually mature from about 50 mm (Hulley 1984). In the Atlantic the species has been found to spawn south of the Polar Front in late winter-early spring, while in the Mediterranean the spawning can continue at low level until summer (Hulley 1984).

1.2.4.3.4 Feeding

Feeds on copepods, euphausiids, zoea stages of Brachyura and fish fry (Hulley 1984).

1.2.5 *Myctophid ecology discussion*

The myctophid species here reviewed are an important part of the oceanic mesopelagic ecosystem in the subpolar-temperate areas of the North Atlantic Ocean. Diet composition and abundance estimates show that the more abundant species like *Benthosema glaciale* are important zooplankton consumers that make a valuable-energy transfer link to predators at higher levels in the food web. Copepods are the most important prey for all those myctophid species, at least for younger age groups, although euphausiids, amphipods and other larger organisms also become important for larger individuals. Myctophids undertake obvious diel vertical migrations, and there are indications of depth stratification at both species and ontogenetic levels. Some studies have shown distinct diurnal feeding cycles, mainly supporting increased nocturnal feeding activity, but others have not.

In general there seems to be opportunistic prey selectivity. Hence the mesopelagic environment appears to favour the zooplankton-eating fish that grabs the next suitably sized prey item that comes in sight. But this assumption must be taken with care, because most of the published investigations on the feeding of these species are lacking the necessary data resolution for applicable selectivity inspection. In addition to the basic variables like individual count of prey in the diet and abundance in the environment, several other factors must be thoroughly investigated to obtain usable data for selectivity studies, e.g. identification of prey developmental stages, sex, prey/predator distribution (in space and time) and morphology. For example, identification of developmental stages in the zooplanktic prey is essential because

there can be strong selectivity for certain developmental stage that might not be evident when combining all stages. There are examples of seasonal foraging changes e.g. *B. glaciale* in Norwegian waters feeds mainly on copepods in summer but during winter euphausiids become an important part of the diet.

Growth rate, maximum age and maximum length vary between Myctophid species. *Notoscopelus e. kroeyeri*, for example, has been found to have higher growth rate than *Benthosema glaciale*. Length distributions usually show only the first one or two year classes, possibly because the extended spawning season serves to merge later modes. Annual changes in growth rate have been observed, e.g. *Benthosema glaciale* in the Rockall Trough. In that area *B. glaciale* has shown seasonal growth variability, growing faster in the summer, most likely due to increased food availability. Differences in growth rate, maximum length and age between areas have been suggested, but lack of data and standardized procedures make such comparison difficult.

There is generally limited information on gonad development and reproduction, but it can be reasoned that *B. glaciale* spawns from March to July. The spawning period varies according to area and environment, and progressions of spawning peaks within spawning populations have been observed. For all species non-spawning (expatriated) population parts are commonly observed outside their habitat. This is usually explained by drift from the species habitat area emphasising the importance of surface and midwater current gyres in maintaining those high-oceanic spawning stocks.

From the studies drawn together here it can be seen how discrete and limited information is available on those species. Ecological research on myctophids and

other mesopelagic fishes has suffered from a lack of the most simple and descriptive information, like abundance, size structure, prey and predators, and hence further ecological modelling has been limited. Back in 1977 Hopkins and Baird stated that "research in virtually all phases of the trophic ecology of midwater fishes is in its initial stages" (Hopkins & Baird 1977) and today this statement still holds, at least concerning myctophids. The few studies that have been made since then have not been as extensive and detailed as one might have expected. Most likely the strongest limitation in the mesopelagic research is the high cost of exploring the depths of the open oceans, but recently there have been technical improvements concerning the exploration of the mesopelagic ecosystem, e.g. in acoustical post processing methods, usage of advanced opening-closing trawls and submersibles.

1.3 Acoustics – theoretical background

Underwater sound consists of waves which propagate long distances through the water. The physics of the sound wave propagation can be used for detection of underwater objects. As mentioned before, this makes underwater acoustics highly important in estimation of abundance and distribution of fish and other components of the underwater ecosystem (Bodholt 1991; Medwin & Clay 1998; Simmonds & MacLennan 2005).

The underwater sound is subject to scattering, reflection and absorption.

1.3.6 *Sound waves*

The transducer vibrates and creates alternating high and low pressure zones (the sound waves). The zones propagate outwards through the water from the transducer where the pressure changes cyclically with distance from the transducer:

$p = \sin(kx)$

Where p = pressure, k = wavenumber and x = distance. Hence the wave-fronts repeat at intervals of the wavelength ($\lambda = 2\pi/k$ where λ = wavelength (m)) as they propagate at sound velocity. The sound velocity describes the speed of the wave-fronts (pressure peaks) as they travel from the source and is the product of wavelength and frequency (Bodholt 1991; Simmonds & MacLennan 2005):

$c = \lambda * f$ (eq. 1)

Where f = frequency (Hz) and c = sound velocity (m/s). Hence, wavelength and frequency are inversely dependent, so that shorter waves will concur with higher frequencies at a fixed velocity. Sound velocity is generally around 1500 m/s in water, depending on temperature, ambient pressure and salinity. This sound speed gives wavelength of 5 cm at frequency of 30 kHz but 1.25 cm at 120 kHz. Frequency f is the number of maxima (wave-fronts) passing in one second, hence:

$T = 1/f$ (eq. 2)

Where T = period = the time between two maxima in a wave (s). In practice the echosounder transmits the sound waves in short pulses comprising a number of periods, described by:

$\tau = n * T$ (eq. 3)

Where, τ = pulse duration (s), n = number of periods in one pulse and T = period. The length of the propagating pulse becomes:

Pulse length = $c * \tau$ (eq. 4)

Importantly the distance between two point targets needs to be more than ½ the pulse length to distinguish between their echoes (Figure 16).

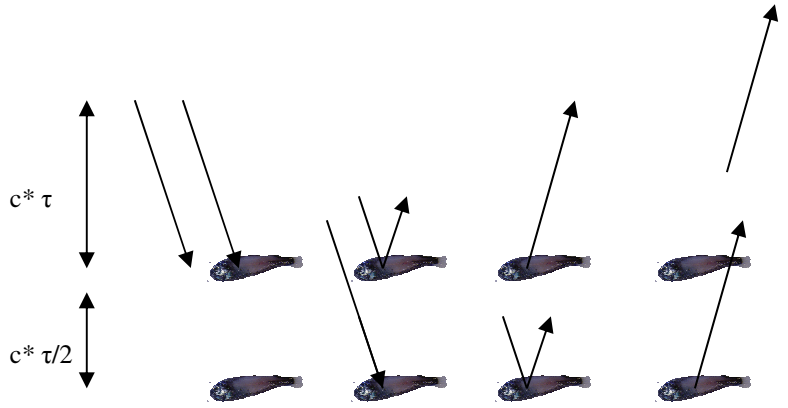

Figure 16 Incident pulse and its separated echoes scattered from fish targets that are more than ½ pulse length apart (adapted from Bodholt (1991)).

1.3.7 *Sound pressure (p) and Intensity (I)*

Sound pressure and intensities are specified by the Pascal (Pa) according to the International System of units (SI) where 1 Pa = 1 N/m^2 with the base units of $kg*m^{-1}*s^{-2}$. For underwater sound pressure levels the µPa (10^{-6} Pascal) is commonly used (e.g. SL, noise etc.).

Sound intensity (I) is the energy passing through a unit area per second described by W/m^2 = $J/s/m^2$ with base units: $kg*s^{-3}$.

$$I = \frac{p^2}{\rho \cdot c} \qquad \text{(eq. 5)}$$

Where I = Intensity (W/m^2), p = pressure (Pa) , ρ = water density (kg/m^3) and c = speed of sound in water (m/s).

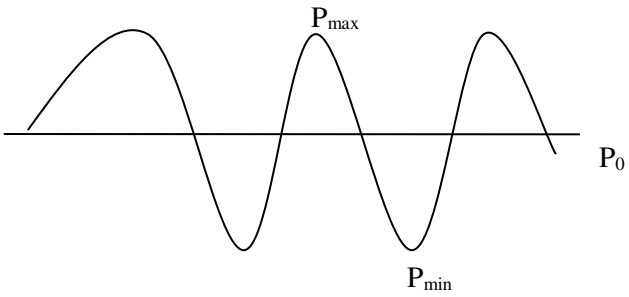

Figure 17 Properties of a pressure wave.

There are 3 ways to quote pressure amplitude: peak-to-peak, peak or RMS (Root-Mean-Square).

$I_{rms} = I_{peak} / 2 = I_{peak\text{-}peak} / 4$ (eq. 6)

$I_{peak\text{-}peak} = P_{max} - P_{min}$ (eq. 7)

$I_{peak} = P_{max} - P_0$ (eq. 8)

Here RMS (p_{rms}) is the square root of the mean of $(P(t) = P_0)^2$ where P(t) is the absolute pressure that cycles between P_{max} and P_{min}. In general it is best to use the RMS measure when energy, power or intensity is expressed in dB referred to a base level including pressure. MRS is usually used to describe man-made sonar transmissions while peak-peak is often used for dolphin sonar transmissions (Simmonds & MacLennan 2005).

1.3.8 *Decibel*

In acoustic observations the sound level can range over many orders of magnitude. Hence, the sound pressure and intensities are commonly expressed within modest range of decibels (dB). The decibel is derived from a logarithm (base 10) of the ratio of two sound intensities I_1 and I_2.

$$n = 10\log\left(\frac{I_2}{I_1}\right) \qquad \text{(eq. 9)}$$

Where n is the number of dB, I_2 = the measured Intensity and I_1 = the reference level of intensity. This implies that a dB value is meaningless unless the reference value is quoted further the defination of pressure amplitude measurements needs to be stated as described above (Simmonds & MacLennan 2005). The decibel equation for sound pressure is derived from eq. 5 and 6 :

$$n = 10\log\left(\frac{I_2}{I_1}\right) = 10\log\left(\frac{(p_2)^2 \big/ \rho \cdot c}{(p_1)^2 \big/ \rho \cdot c}\right) = 20\log\left(\frac{p_2}{p_1}\right) \qquad \text{(eq. 10)}$$

Where p_1 = the reference pressure and p_2 = the measured pressure.

1.3.9 *Sonar equation:*

The energy budget of the propagating sound wave is a key element behind biomass estimates from the active sonars commonly used by fisheries scientists. The transducer of the echosounder used in stock assessments converts electrical energy into acoustic pulse and later converts the reflected echoes from underwater targets to electrical signals. The two way budget of the transmitted acoustic source level and the received echo level (in dB relative to 1 μPa) given proper knowledge of the

physics of the propagating sound wave and the properties (target strength) of the scattering target can by summarised by the following formula (see e.g. (Johannesson & Mitson 1983; Bodholt 1991; Simmonds & MacLennan 2005):

$$EL = SL - 2\,TL - TS + G \qquad \text{(eq. 11)}$$

Where EL = Echo Level (or SPL = Sound Pressure Level), SL = Source Level, TL = Transmission Loss, TS = Target Strength and G = Gain.

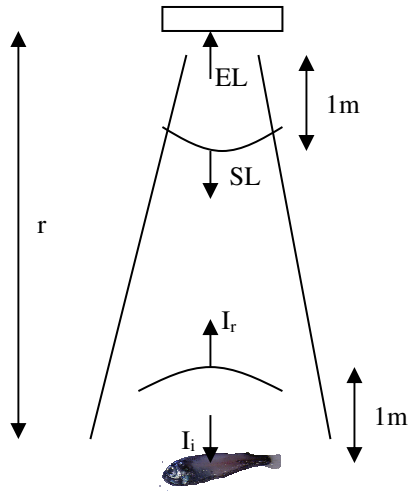

Figure 18 Some parameters involved in the energy budget of the incident and backscattered waves of the acoustic beam (adapted from Johannesson and Mitson (1983).

1.3.9.1 Echo Level (EL)

The echo level (EL) describes the received pressure or Intensity at the transducer, such that the dB value becomes:

$$EL = 10\log\left(\frac{|p_r|^2}{(1\mu Pa)^2}\right) \qquad \text{(eq. 12)}$$

Where, p_r is the pressure of the received wave at the transducer.

1.3.9.2 Source Level (SL)

The source level (SL) is the sound pressure in the transmitted pulse at the beam axis 1 m from the transducer.

$$SL = 10\log\left(\frac{p_i{}^2 r^2}{(1\mu Pa)^2 (1m)^2}\right)$$

(eq. 13)

$$SL = 10\log\left(\frac{p_i}{(1\mu Pa)}\right)^2 = 20\log\left(\frac{p_i}{(1\mu Pa)}\right)$$

Here, pi is the pressure of the initial wave at the 1 m range (r).

1.3.9.3 Transmission Loss (TL)

Geometrical spreading and absorption cause Transmission Loss of the propagating wave.

1.3.9.3.1 Geometrical spreading

The intensity decreases with the square of the range due to spherical spreading in the far field of the transmitted beam. The far-field is where the wave fronts have propagated far enough from the transducer elements so that their wave fronts are parallel. The near-field (defined by the transducer diameter and wavelength) is the region immediately in front of the transducer where intensity has complicated range dependence.

Given no loss in the medium, the power generated by the source is radiated equally in all directions. Hence wave fronts form spheres. The power P stays the same while sphere surface increases.

Power equals intensity times area:

$P = 4 \pi r_1^2 I_1 = 4 \pi r_2^2 I_2$ (eq. 14)

Where r_1 and r_2 are the radii of two spheres and I_1 and I_2 are the sound intensities at these radii. Hence the ratio between the two intensities is:

$$\frac{I_2}{I_1} = \frac{r_1^2}{r_2^2} \quad \text{(eq. 15)}$$

Expressed in dB the geometrical spreading becomes:

$$TL_s = 10\log\left(\frac{I_1}{I_2}\right) = 20\log\left(\frac{r_2}{r_1}\right) \quad \text{(eq. 16)}$$

and with r_1 set to reference distance of 1 metre the one way spreading loss is:

$TL_s = 20 \log r$ (eq. 17)

While two way spreading becomes:

$TL_s = 40 \log r$ (eq. 18)

1.3.9.3.2 Absorption

When the sound wave propagates through the water, part of the wave energy is absorbed by the water and converted to heat.

For each metre a certain fraction of the sound intensity is lost.

$TL_a = \alpha r$

Where, α = absorption coefficient, and r = range. For accurate equations see Francois and Garrison (1982b; 1982a). The absorption is mainly determined by the frequency, but also affected by temperature and salinity (Simmonds & MacLennan 2005).

1.3.9.3.3 Total Transmission Loss

Total one way transmission from the spreading (TLs) and absorption (TLa) in dB becomes:

$TL = TL_s + TL_a = 20 \log(r) + \alpha r$ (eq. 19)

While two way transmission loss becomes:

$2 * TL = 40 \log(r) + 2 \alpha r$ (eq. 20)

1.3.10 *Target Strength (TS)*

The target strength is a logarithmic measure of the proportion of the incident energy which is backscattered by the target (Simmonds & MacLennan 2005).

1.3.10.1 Backscattering cross-section (σ_{bs})

The backscattering cross-section (σ_{bs}) describes the strength of backscattering and is defined in terms of the intensities of the incident and the backscattered waves (Simmonds & MacLennan 2005).

$$\sigma_{bs} = R^2 \frac{I_{bs}}{I_i} \quad \text{(eq. 21)}$$

Where, σ_{bs} = backscattering cross-section (m^2), R = distance (range) (m) of the measured intensity from the target, I_i = Intensity of the incident waves at the target and I_{bs} = Intensity at the midpoint of the backscattered pulse. I_{bs} depends on the distance R from the target while R needs to be out of the near field of the target, but within the limits defined by absorption. Since the spreading loss of I_{bs} is squared the ($R^2 I_{bs}$) becomes the same at all ranges and σ_{bs} is constant for the given target (Simmonds & MacLennan 2005). For convenience the differential backscattering

cross-section is commonly represented logarithmically as target strength (TS) in decibel units:

$$TS = 10 \log (\sigma_{bs}) \qquad \text{(eq. 22)}$$

A 3 dB difference between target strength of two targets implies that the weaker target scatters half the energy of the stronger scatter (Simmonds & MacLennan 2005).

1.3.11 *Beam pattern*

The transmit response (acoustic level) and receive response (echo level) are highest along the beam axis, so echoes received from a target will decrease as it is located more off axis. Hence, echo amplitude of a target depends on the target strength of the fish and its position in the beam. The transducer beam width is commonly described by the angle between opposite sides of the main lobe where the intensity is 3 dB less than on axis (Simmonds & MacLennan 2005).

The equalent beam angle (ψ) also known as the reverberation angle is the solid angle at the apex of an ideal conical beam where the beam pattern (b) equals 1 inside but 0 elsewhere. This ideal beam would give same echo-integral (S_v) as all targets within the actual beam including side lobes (side lobes are usually < 1% of transmitted energy). The equivalent beam angle is in steradians and defined as (Simmonds & MacLennan 2005):

$$\psi = \int_{\theta=0}^{\pi} \int_{\phi=0}^{2\pi} b^2(\theta,\phi)\sin(\theta)\, d\theta\, d\phi \qquad \text{(eq. 23)}$$

Where, θ and ϕ are angles in spherical polar coordinates that determine a point (P) relative to the transducer origin (O). θ is the angle of OP from the acoustic axis, ϕ is the azimuthal angle of OP projected onto the transducer face and b is the beam pattern. The equivalent beam angle described on logarithmic scale becomes EBA = 10 log(ψ) in dB re 1 steradian.

1.3.12 *Acoustic backascatter as fish stock estimate*

Fish stock estimates from acoustic-survey data are based on the allocation of backscattered sound energy to species (Simmonds & MacLennan 2005). Expert scrutiny of echograms in conjunction with data from trawl hauls is used traditionally to link echoes to species, and species identification is one of the main challenging factors and a limit to the ultimate accuracy of a survey (Petitgas & Levenez 1996; Horne 2000; Gauthier & Horne 2004). Trawl data collected in conjunction with acoustic surveys can aid identification, but trawl catch data have several limitations in terms of acoustic interpretation, including species selectivity of fishing gear, the discrete and other distant nature of net samples, and interpolation effects (Doonan *et al.* 2003; O'Driscoll 2003; Gauthier & Horne 2004). A variety of techniques have been used in discrimination and identification of constituent species within acoustic data to overcome these limitations, including modelling for the acoustic backscatter based on the morphology of the fish body and swimbladder (Andreeva 1964; Love 1978; Furusawa 1988; Chu *et al.* 1993; Stanton *et al.* 1993; Kloser *et al.* 2002; Lavery *et al.* 2002). We seek to use modelling approaches here to aid acoustic identification and discrimination of a poorly-known but likely ecologically-important group in the mesopelagic north Atlantic.

1.3.13 *Target strength*

Knowledge of the target strength (TS) of the individual fish targets that are contributing to the received acoustic signal is essential for calculation of numerical abundance and biomass estimates (Simmonds & MacLennan 2005). There is, however, a general lack of information on the backscattering properties of myctophids and other mesopelagic fish in the northeast Atlantic. Mamylov (1988) estimated TS_{38}

$_{kHz}$=25.2 log10(SL) -75.0 where SL = standard length (the length from the tip of the snout to the base of the caudal fin), for myctophids, mainly *B. glaciale* and *Ceratoscopelus maderenis*, in the northwest Atlantic based on *in situ* acoustic observations at 38 kHz and net sampling. Torgersen and Kaartvedt (2001) used split-beam echo target tracking in near surface waters of a Norwegian fjord to study *in situ* swimming behaviour of *Maurolicus muelleri* and *Benthosema glaciale*. They estimated the TS of 5.4 cm mean length *B. glaciale* to range from about -54 to -69 dB at 38 kHz. In a similar swimming behaviour study in a nearby fjord, Kaartvedt *et al.* (2009) tracked ascending and descending targets within the TS range of -62 to -52 at 320-370 m depths with an upward-facing echosounder. Within four target groups which they ascribed to *B. glaciale* (6 cm mean length) they found median TS values ranging from -60.3 to -58.9 dB at 38 kHz. Hence, the upper range of the $TS_{38\ kHz}$ estimates by Torgersen & Kaartvedt (2001) and Kaartved *et al.* (2009) coincided with the estimates by Mamylov (1988). Other studies have been conducted on backscatter of myctophids and similar mesopelagic fish beyond the Atlantic (Koslow *et al.* 1997; Benoit-Bird & Au 2001; Yasuma *et al.* 2003; Yasuma *et al.* 2006; Yasuma *et al.* 2009), usually finding lower $TS_{38\ kHz}$ than predicted by the commonly used TS-length relationship (TS_{38} = 20 log(Length) – 67.5) for physoclists (Foote 1987) but the physoclistous swimbladder (as in adult myctophids) is without any connection to the gut. Those studies described myctophid species with and without air in the swimbladder and furthermore in some cases proportional reduction of air volume with fish size was described. Such variability in morphology and properties of swimbladders among and within myctophid species has been suggested to be adaptation to different vertical migration patterns where fish that have greater depth range are believed to benefit from reduction or even disappearance of air in the

swimbladder (Bone & Marshall 1982; Bond 1996). Even though myctophids have been observed to have relatively large gill surface and well adapted gas gland and oval organ for efficient secretion and absorption of gas to maintain the swimbladder volume the vertical migrations might require to much oxygen demand during more extreme depth ranges (Marshall 1960). Air reduction in the swimbladder is caused by deposition of lipids between the peritoneum and tunica externa while further fat investment in the myctophid body is needed to compensate for the reduced buoyancy by air (Marshall 1960).

In this study we take initial steps towards estimating the TS of 3 important myctophid species *Benthosema glaciale*, *Notoscopelus kroeyeri* and *Myctophum punctatum* that are abundant in sub-polar and temperate areas of the northeast Atlantic (Backus & Craddock 1977). We used soft x-ray technology to visualize and measure dimensions of air inclusions in the swimbladder. Theoretical estimates of TS were made using a prolate spheroid (PS) model for swimbladders and a distorted wave Born approximation (DWBA) model for fish bodies. Further we used a simple spherical (SS) model to estimate occurrences and consequences of targets being in Rayleigh or resonant scattering regions where TS peaks rapidly with frequency.

1.3.13.1 Target strength estimation

The back scattering cross section or target strength can be estimated experimentally or/and theoretically for an acoustic group e.g. fish species. The estimates can be made directly *in situ* by converting acoustic measurements of fish in their natural environment to target strengths. This approach requires species identification of the insonified fish along with knowledge on quantity and size distribution (Foote 1991; Simmonds & MacLennan 2005). Further, the tilt distribution of the insonified targets

must be representative for the unbiased average of the stock component being quantified otherwise the tilt of single targets needs to be observed so the angle related TS estimates can be adapted to a naturally occurring distribution of tilt angles. For mesopelagic fish like myctophids it is very difficult to evaluate the necessary parameters due to depth and gear avoidance. *Ex situ* experiments can also be used where the fish are taken out of their natural environment and kept in a controlled environment, e.g. free swimming in a cage or immobilized and unconscious, while their acoustic backscatter from an echosounder is observed. Further, theoretical acoustic scattering models can estimate TS in relation to the function of stochastic variables like size, shape, body condition, environment and acoustic frequency.

1.3.13.2 Theoretical TS models

Several types of theoretical scattering models have been adapted to estimate the TS of fish such as T-matrix method (Waterman 1969), some straight and deformed cylinders models (Stanton 1989; Ye 1997b), Kirchoff approximations (Clay & Horne 1994), spherical models (Anderson 1950), prolate spheroid models (Furusawa 1988; Chu *et al.* 1993; Stanton *et al.* 1993; Kloser *et al.* 2002; Lavery *et al.* 2002), Fourier mode matching (Reeder & Stanton 2004) and boundary element method (Foote and Francis 2002) and finite element method (Lilja *et al.* 2004) as summarised in (Macaulay et al 2013). Further there have been some developments of models like the Distorted wave Born approximation (DWBA) for estimates of TS from weak scatterers like zooplankton e.g. (Smith *et al.*; Amakasu & Furusawa 2006; Lawson *et al.* 2006) and fish without swimbladder (Gorska *et al.* 2005).

The vacant prolate spheroid model described by Furusawa (1988) has previously been used to estimate TS of the myctophid *Diaphus theta* based on swimbladder measurements (Yasuma *et al.* 2003).

If the frequency of the acoustic wave is close to the natural oscillation frequency of the swimbladder it is said to resonate, resulting in a lot stronger backscatter than at other frequencies (Simmonds & MacLennan 2005). This can result in positively biased estimates of fish biomass in acoustic surveys when the echosounder frequency is near the resonance frequency of the fish swimbladders. Further, this can cause temporal and spatial variations in frequency response of the backscatter, affecting multi-frequency target identification (Godo *et al.* 2009) and precision of surveys.

We chose the DWBA model (Chu *et al.* 1993; Stanton *et al.* 1993; Lavery *et al.* 2002) to estimate TS from the morphology and physical properties of the fish body. The DWBA model has mainly been used on zooplankton (Stanton & Chu 2000; Simmonds & MacLennan 2005) as it is limited to weak scatterers where sound speed and density in the target body must be close to corresponding values in the surrounding water. Airless myctophids have been found to fulfil those requirements (Yasuma *et al.* 2006) and hence the DWBA model was considered to be suitable for the myctophid body.

To the best of our knowledge we present here the first length related multifrequency estimates of TS for *B. glaciale, N. kroyeri and M. punctatum*. Our data span the common fisheries research frequencies. Further we present new data on the physical properties and morphology of the swimbladder of those species, particularly interesting in the special case of *B. glaciale* that has variable air content with size.

2 MATERIALS AND METHODS

2.1 Sampling

The three myctophid species were collected from the Irminger sea during two cruises on the research ship Arni Fridriksson. In June-July 2005 a large midwater trawl (60 m vertical opening and 9 mm mesh size in the codend) was towed horizontally at a depth of 400 m, and in November 2006 another midwater trawl (45 m vertical opening, 9 mm mesh size in codend) was towed horizontally at depths between 50-100 m and retrieved with slow heaving. Samples were sorted and frozen immediately to -25°C (first cruise) or flash frozen with liquid nitrogen (second cruise) and stored at -25°C.

2.2 Swimbladder and body morphology

The frozen fish samples were transported to a laboratory at the Research Institute of Fisheries Engineering in Japan where the samples were thawed in cold water and then each individual fish was scanned with a soft X-ray analysing system (SOFTEX PRO-TEST 100).

Soft X-rays are weak X-rays with wavelengths from 10^{-8} to 10^{-10} m. The image is based on the difference in the amount of penetrating versus absorbed X-ray energy (Nagai 2003). Penetrating power (voltage) and cumulative dose (amperage * time) were adjusted while magnified live video footage was observed. This enabled for precise scanning for any air-bubbles within the specimen. Still images were captured and exported at 640x480 pixels resolution (Figure 20), then calibrated and measured in SigmaScanPro5 image analysis software. When an air-bubble was present in the swimbladder, its major-axis, minor-axis and the major-axis/body-axis angle were

measured both for lateral and dorsal aspect (Sawada *et al.* 1999; Yasuma *et al.* 2003). Swimbladder volume was estimated as the volume of a prolate spheroid ($V = 4/3\ \pi\ b^2\ a$), where a and b are the semi-major and semi-minor axes respectively. Air inclusion of the swimbladder was then confirmed with dissection and, occasionally, an additional soft X-ray scan of the removed swimbladder.

External morphology of the fish body was measured using digital image analysis. Each fish was photographed in lateral and dorsal aspect using a Canon EOS Kiss Digital N camera. The 8 megapixel images were calibrated against a graduated background and then measurements of standard-length (SL), height and width of the fish were made with SigmaScanPro5.

2.3 Theoretical models for TS.

Backscatter from the fish body was estimated with the DWBA model while backscatter intensity from the swimbladder was estimated using a prolate spheroid adapted resonance scattering model (RSM). We summed contributions of body and bladder to give total fish backscatter. According to Gorska & Ona (2003) the backscattering cross-section of the whole fish (σ_{bsc}) can be estimated as;

$$\sigma_{bsc} = \sigma_{sb} + \sigma_b + \sigma_{in} \qquad \text{(eq. 24)}$$

where σ_{sb} and σ_b are the backscattering cross-sections of the swimbladder and body, respectively and σ_{in} accounts for the contribution of echo interference. We reduced the equation to;

$$\sigma_{bsc} = \sigma_{sb} + \sigma_b \qquad \text{(eq. 25)}$$

because in *B. glaciale* we found that the vertical spatial displacement between the centres of the air bladder and the body was negligible and at all frequencies it is much shorter than $\lambda/2$, even at 200 kHz where λ is only 7.5 mm and hence interference is unlikely at the frequencies we seek to model for practical application (18, 38, 70, 120 and 200 kHz). As the RSM model accounts for resonance, possible effects of resonance on TS were investigated and compared to an exact solution model (ESM) as another exact soulution model (PSVM) was used for visualisation of the backscattering pattern at different tilt angles.

2.3.14 *Plorate spheroid void model (PSVM)*

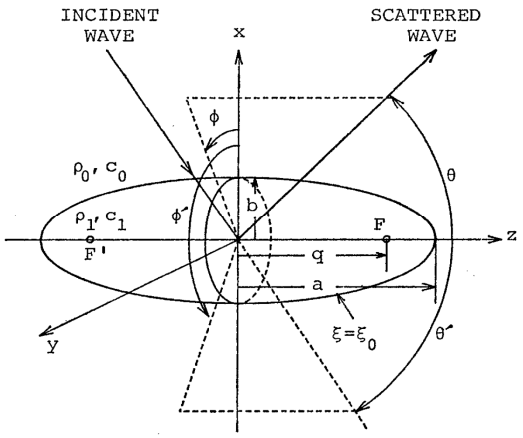

Figure 19 A prolate spheroid drawn on prolate spheroidal coordinates where the spheroid surface is given by $\xi = \xi_0$ = constant. a = major radius, b = minor radius, q = semi-focal-length. ρ = density, c = sound speed, k = wavenumbers. Subscripts 1 for body and 0 for surroundings(Furusawa 1988). Other parameters are described in the text.

This exact soulution model estimates the backscatter from a vacant prolate spheroid (Furusawa 1988) and is in this study only used to describe possible tilt patterns of the swimbladder target strength, i.e. how the backscatter is likely to change as the tilt of swimbladder changes away from broadside aspect of the incident beam. In this model

the far field scattering amplitudes of prolate spheroids are determined by solving the scalar wave equation in spheroid coordinates:

$$f_{\infty}(\theta,\phi|\theta',\phi') = \frac{2}{jk_0}\sum_{m=0}^{\infty}\sum_{n=m}^{\infty}\frac{\varepsilon_m}{N_{mn}(h_0)}S_{mn}(h_0,\cos\theta')\times A_{mn}S_{mn}(h,\cos\theta)\cos m(\phi-\phi')$$

(eq. 26)

and applying the boundary conditions for a soft spheroid:

$$A_{mn} = \frac{-R_{mn}^{(1)}(h_0,\xi_0)}{R_{mn}^{(3)}(h_0,\xi_0)} \qquad \text{(eq. 27)}$$

where θ, ϕ and θ′, ϕ′ are the spherical angle coordinates of the scattered and incident waves respectively, $j=(-1)^{1/2}$, k_0 is the wave number, ε_m is the Neumann function, N_{mn} is the norm, S_{mn} is the angle prolate-spheroid wave function of first kind of order *m* and degree *n*, A_{mn} is the expansioyn coefficient for the scattered wave, and R is the radial spheroid wave function of the i-th kind. It was assumed that the myctophids maintain constant air-volume in their physoclistous swimbladders at all depths (Benoit-Bird *et al.* 2003; Yasuma *et al.* 2010).

2.3.15 *Exact solution scattering model (ESM) (Anderson model)*

Anderson (1950) presented exact solution scattering model for the scattering of sound from a fluid sphere surrounded by an external fluid with different density and sound speed properties. This model can be applied, over a wide frequency range, to an air bubble surrounded by seawater by using sound speeds and densities of air and seawater representing the internal and external medium respectively (Medwin & Clay 1998; Feuillade & Clay 1999). Here, the backscattering of the myctophid swimbladder was estimated by this model using the radius of a sphere having equalent

volume to a prolate spheroid, calculated from the X-ray measured dimensions of the swimbladders.

$$a_{es} = a\left(\frac{a}{b}\right)^{-\frac{1}{3}} \quad \text{(eq. 28)}$$

$$C_m \equiv \frac{\left[\frac{\alpha_m(k'a_{es})}{\alpha_m(ka_{es})}\right]\left[\frac{n_m(ka_{es})}{j_m(k'a_{es})}\right] - \left[\frac{\beta_m(ka_{es})}{\alpha_m(ka_{es})}\right]gh}{\left[\frac{\alpha_m(k'a_{es})}{\alpha_m(ka_{es})}\right]\left[\frac{j_m(ka_{es})}{j_m(k'a_{es})}\right] - gh} \quad \text{(eq. 29)}$$

$$\alpha_m(kr) = mj_{m-1}(kr) - (m+1)j_{m+1}(kr) \quad \text{(eq. 30)}$$

$$\beta_m(kr) = m_{n-1}(kr) - (m+1)n_{m+1}(kr) \quad \text{(eq. 31)}$$

$$g = \frac{\rho'}{\rho} \quad \text{(eq. 32)}$$

$$h = \frac{c'}{c} \quad \text{(eq. 33)}$$

$$R = \frac{2}{ka}\left|\sum_{m=0}^{\infty}\frac{P_{m(\mu)}(-1)^m(2m+1)}{1+iC_m}\right| \quad \text{(eq. 34)}$$

$$\sigma_{bs} = a^2\frac{R^2}{4} \quad \text{(eq. 35)}$$

$$TS = 10\log_{10}(\sigma_{bs}) \quad \text{(eq. 36)}$$

Where, a_{es} = radius for equivalent spherical bubble, a = minor semi-axis, b = major semi-axis, $k = \omega/c$ = the propagation wave number, where ω is the angular frequency of incident waves, m = order of terms of spherical normal modes, p_m = the Legendre function, j_m = spherical Bessel function, n_m = spherical Neumann function, ρ = density, c = sound speed, the term ′ stands for values in the fish body, σ_{bs} =

backscattering cross section and *TS* = target strength. Calculations were made using the R statistics software (R-Core-Team 2014) and values of the Legendre function were evaluated by the "legendre" function within the "prackma" R package (Borchers 2014). The spherical functions, j_m and n_m were evaluated by the R-base functions "besselJ" and "besselY" respectively.

2.3.16 *DWBA*

To estimate the backscattering properties of the fish body we used the following DWBA derived equation (for details see Chu *et al.* (1993), Stanton *et al.* (1993) and Lavery *et al.* (2002)):

$$TS_{DWBA} = 20Log_{10}\left|\frac{ABC}{D^2}\left(\frac{1+h^2-2gh^2}{g}\right)\left(\frac{\sin k'D}{k'D}-\cos k'D\right)\right|$$

$$D = 2\sqrt{\left(A\sin\theta\cos\psi\right)^2+\left(B\sin\theta\sin\psi\right)^2+\left(C\cos\theta\right)^2} \qquad \text{(eq. 37)}$$

where A, B and C are the semi-major axis lengths (m), vertical semi-minor axis and horizontal semi-minor axis of the fish body respectively, h=c′/c (where c′=1520 m/s and c=1480 m/s) , c=speed of sound, g=ρ′/ρ (where ρ′=1035 kg/m^3 and ρ=1027.52 kg/m^3), ρ=mass density, k′=2πf/c′, f=frequency, θ=tilt angle of target, ψ=roll angle of target. The term ′ stands for values in the fish body. For this model we calculated the mean sound speed and density of seawater for the upper 500 m in Irminger Sea based on CTD measurements made from the research vessel Arni Fridriksson in June-July 2003. For sound speed and density of the fish body we used the values from Yasuma *et al.* (2006) measured at the same temperature for the myctophid *S. leucopsarus*. Sound speed in seawater was calculated following the equation described by Mackenzie (1981).

For all models the calculated mean TS of each individual fish was weighted by Gaussian probability distribution of tilt angles with mean of 0° and standard deviation of 15°. In this study all calculations of mean TS and its 95% confidence intervals were made on the backscattering cross-section (σ_{bs}), i.e. in the linear domain.

2.3.17 *Resonance scattering model (RSM)*

Backscattering properties of swimbladders containing air were estimated by a model adapted for prolate spheroids (for details see Andreeva (1964), Weston (1967), Love (1978) and Ye (1997a). Here the approach of Ye (1997a) was followed with addition of thermal and viscous damping terms given by Love (1978). In this model the theory of spherical backscatter is adapted to account for the effect of the prolate spheroid shape and the slight increase in resonance frequency caused by the prolate spheroid shape. Importantly this model accounts for the backscattering effects of resonance influenced by radiation-, viscous- and thermal-damping.

$$\sigma_{bs} = \frac{\left(\frac{\varepsilon b}{\ln\left(\frac{1+\varepsilon}{e} \right)} \right)^2}{\left(\frac{\omega_0^2}{\omega^2} - 1 \right)^2 + \delta^2} \qquad \text{(eq. 38)}$$

$$a_{es} = a e^{-\frac{1}{3}} \qquad \text{(eq. 39)}$$

$$\omega_e = \frac{1}{a_{es}} \sqrt{\frac{3\gamma P_0}{\rho_w}} \qquad \text{(eq. 40)}$$

$$\omega_0^2 = \omega_e 2^{1/2} e^{-1/3} \left(1 - e^2\right)^{1/4} \left[\ln\left(\frac{1+\varepsilon}{1-\varepsilon} \right) \right]^{-1/2} \qquad \text{(eq. 41)}$$

$$e = \frac{a}{b} \qquad \text{(eq. 42)}$$

$$\varepsilon \equiv \sqrt{1-e} \qquad \text{(eq. 43)}$$

$$\delta = \delta_{rad} + \delta_{vis} + \delta_{th}$$
$$\delta_{rad} = kb\left(\frac{\ln\left(\frac{(1+\varepsilon)}{e}\right)}{\varepsilon}\right)^{-1}$$
$$\delta_{viz} = \frac{2\xi}{\rho_f \omega a^2} \qquad \text{(eq. 44)}$$
$$\delta_{th} = \frac{3(\gamma-1)}{\omega a}\left(\frac{\omega\kappa_a}{2\rho_a c_{pa}}\right)^{1/2}\left(1+\frac{2s}{\rho_f \omega^2 a^3}\right)$$

Since this model does not account for changes in backscatter due to tilt of swimbladder, a directivity function ($D(\theta)$) was added (e.g. Urick 1967).

$$D(\theta) = \frac{\sin^2(2kb\sin(\theta))}{(2kb\sin(\theta))^2} \qquad \text{(eq. 45)}$$

$$\sigma_{bs}(\theta) = D(\theta)\sigma_{bs} \qquad \text{(eq. 46)}$$

where, σ_{bs} = acoustic backscattering cross section, ω = angular frequency = $2\pi f$ (where f = frequency), a_{es} = radius for equivalent spherical bubble, ω_e = angular resonance frequency of the equivalent spherical bubble, γ = ratio of specific heats for the swimbladder gas, P_0 = hydrostatic pressure((1+0.103d)10^5)), ρ_w = density of surrounding water, ξ = viscosity parameter, ρ_f = density of fish flesh, κ = thermal conductivity of air, ρ_a = density of air inside swimbladder, c_{pa} = specific heat at constant pressure for air, s = surface tension of swimbladder, ω_0 = angular resonance frequency of the swimbladder, δ = damping factor (where δ_{rad}, δ_{vis}, δ_{th} are radiation-, viscous- and thermal-damping), $D(\theta)$ = directivity function at tilt angle θ. Model

parameters are shown in Table 1. As *B. glaciale* is a very small mesopelagic fish the viscosity parameter ξ of 10 kg/(m sek) was used as it is the lowest value suggested by Love (2013) for mesopelagic fish.

3 RESULTS

3.1 Morphology

The soft X-ray scans indicated that adult *N. kroeyrii* (SL; 4.8-10.1 cm) and *M. punctatum* (SL; 6.4-8.5 cm) did not have air-filled swimbladders while the majority (71%) of *B. glaciale* (SL; 3.2-6.5 cm) had air in the swimbladder (Figure 20).

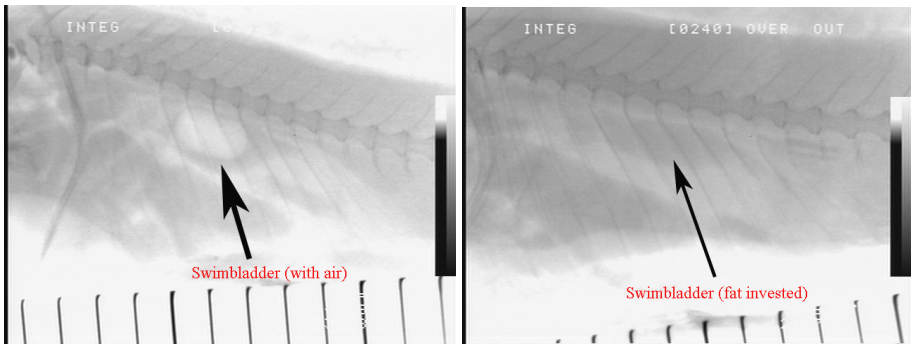

Figure 20. Soft x-ray photo of two *B. glaciale*, with and without air in the swimbladder.

Dissection revealed that a swimbladder was present in all fish and that extensive fat investment in the swimbladder explained the absence of air in *N. kroeyerii*, *M. punctatum* and some *B. glaciale*. The volume of air in the swimbladder of *B. glaciale* was very variable and did not show a significant relationship ($p = 0.3482$) to fish length. Further, there was only a very weak but significant negative relationship ($R^2 = 0.05$, $p = 0.03592$) between the body length and major-axis length of the air bubble in the swimbladder (Figure 21).

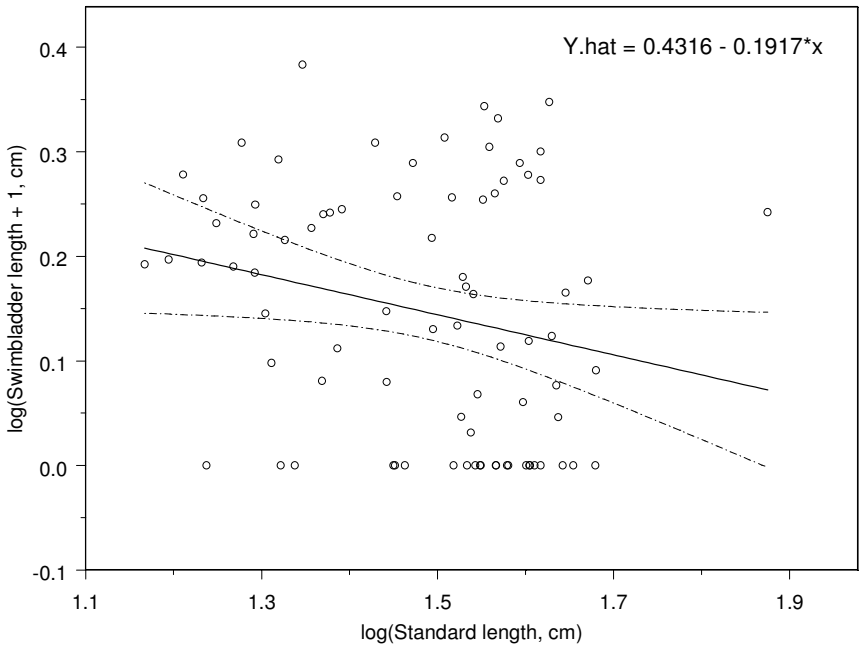

Figure 21 Log(Swimbladder length +1) versus log(Standard length) of *B. glaciale*. Solid line shows regression. Dashed lines show 95% Confidence limits of Y.hat.

3.2 Sound speed and density

In the Irminger Sea in June-July 2003 average values for seawater temperature and salinity in the top 500 m were 6.4°C and 35.04 respectively (Hedinn Valdimarsson unpublished data), resulting in soundspeed (c) and mass density (ρ) of 1480 m/s and 1027.5 kg/m^3 respectively. Measurements from the myctophid *S. leucopsarus* (Yasuma *et al.* 2006) gave sound speed (c′) and density (ρ′) of the myctophid body as 1520 m/s and 1035 kg/m^3 respectively at this temperature. Hence, the sound speed contrast (h=c′/c) was 1.027 and the density contrast (g=ρ′/ρ) 1.007.

3.3 Target Strength

Since *N. kroeyeri* and *M. punctatum* did not have air in the swimbladder, we used only the DWBA model to estimate TS of those species. For *B. glaciale* we used the sum of the backscatter from swimbladder (RSM model) and the body (DWBA model). Figure 22 shows as an example the TS tilt pattern for the body of *M. punctatum* at five frequencies that are common in scientific echosounding.

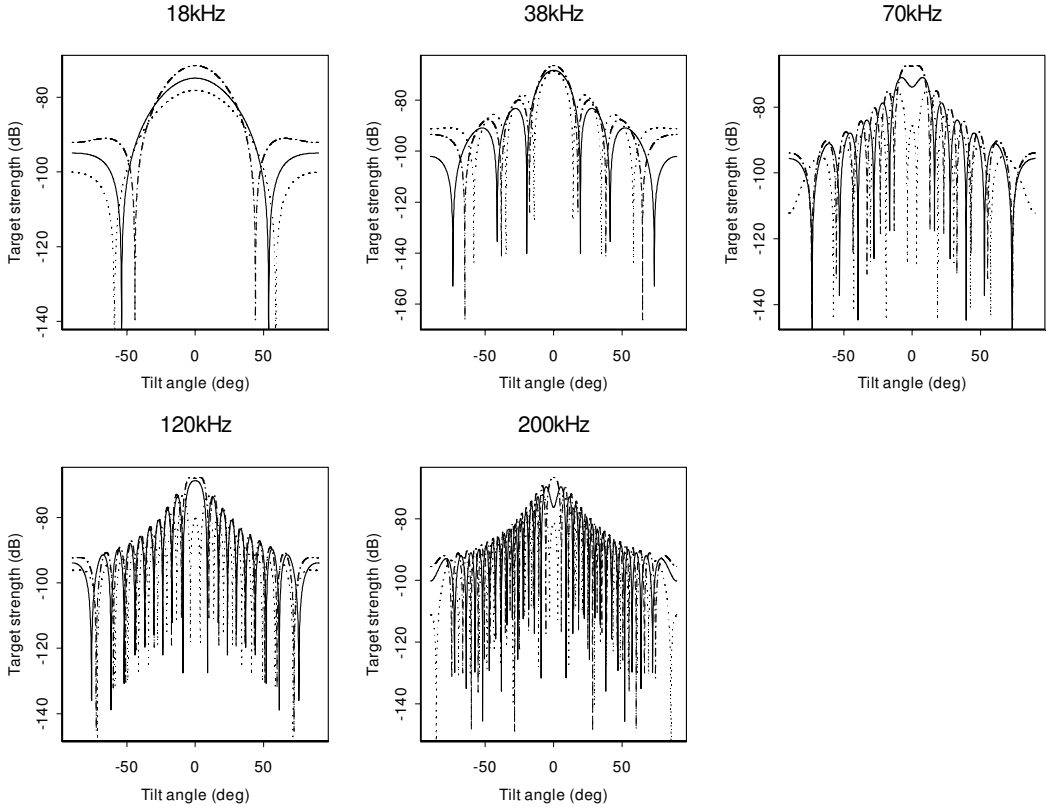

Figure 22 TS pattern for *M. punctatum* estimated with the DWBA model. Dotted, solid and dot-dashed lines show the TS pattern for fish having min, median and max TS values at each frequency.

The RSM derived TS tilt patterns of swimbladders for the *B. glaciale* containing air in the swimbladder (Figure 23) show much less angular dependence, especially at the lower frequencies.

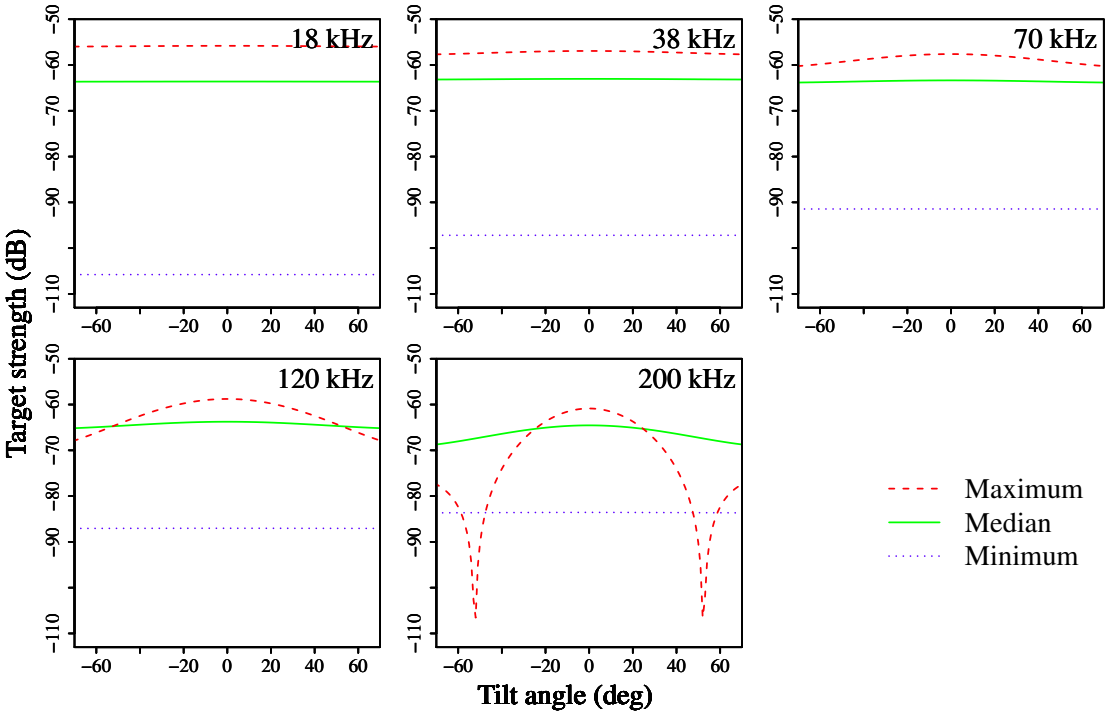

Figure 23 Swimbladder TS pattern for *B. glaciale* with air in the swimbladder, estimated with the RSM model. Dotted, solid and dot-dashed lines show the TS pattern for fish having min, median and max TS values at each frequency.

Figure 24 shows examples of whole fish TS-tilt patterns where backscatters of body and swimbladder have been added together. For visual comparison only, a similar combination of the PSVM and DWBA models is shown in Figure 25, the PSVM model was not used in any mean TS estimates in this study.

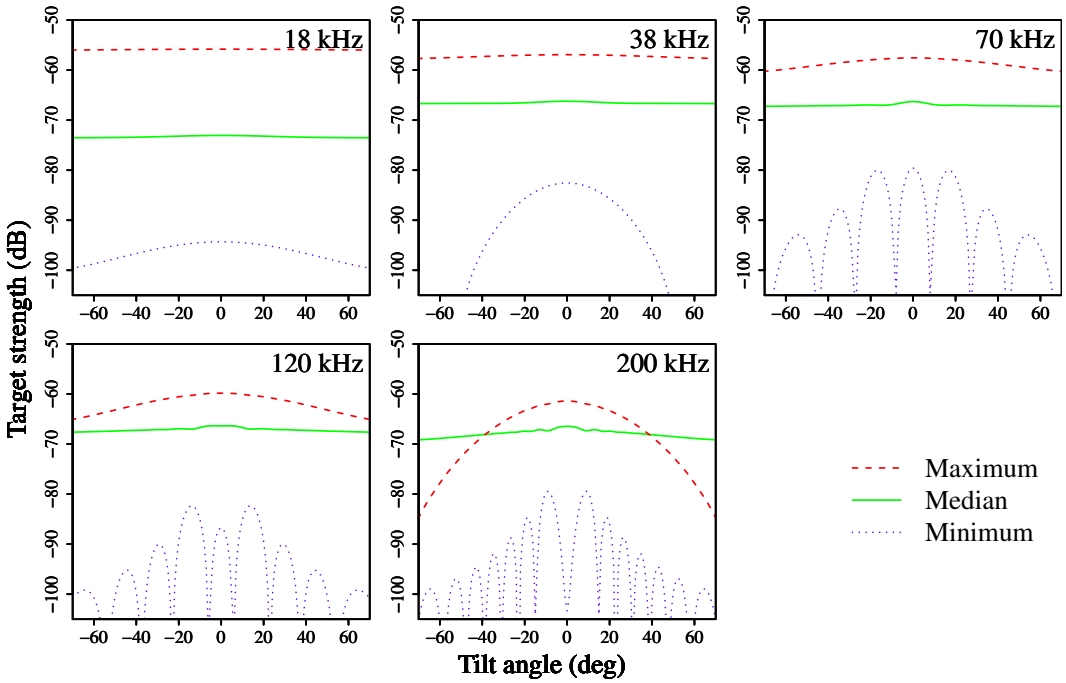

Figure 24 Whole body TS-tilt pattern for *B. glaciale* where the contribution of swimbladder (RSM model) and body (DWBA model) are added together. Dotted, solid and dot-dashed lines show the TS pattern for fish having min, median and max TS values at each frequency.

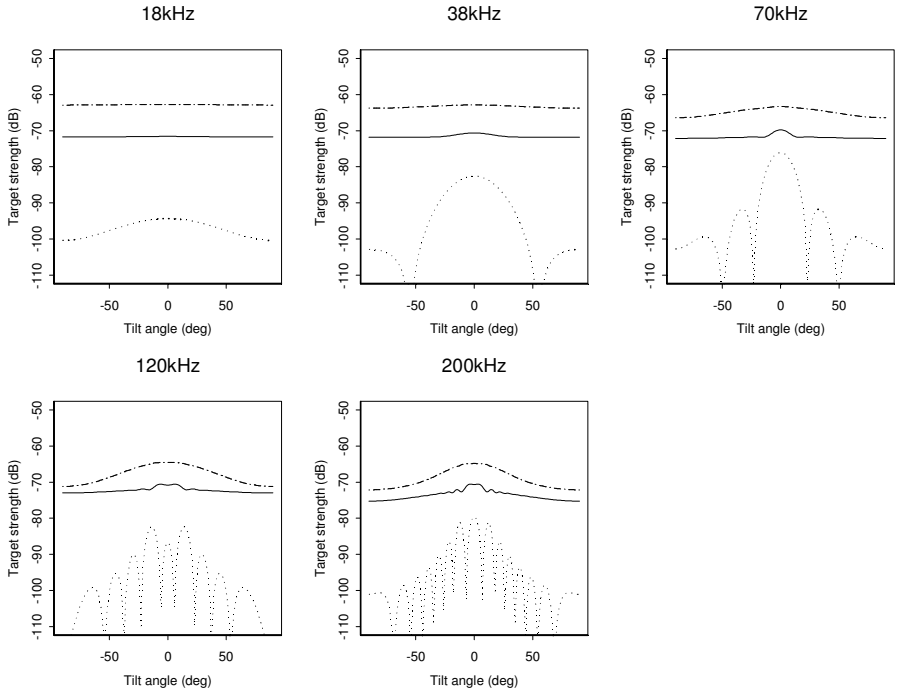

Figure 25 Whole body TS-tilt pattern for *B. glaciale* where the contribution of swimbladder (PSVM model) and body (DWBA model) are added together. Dotted, solid and dot-dashed lines show the TS pattern for fish having min, median and max TS values at each frequency.

The mean frequency dependencies of TS estimates are shown in Figure 26.

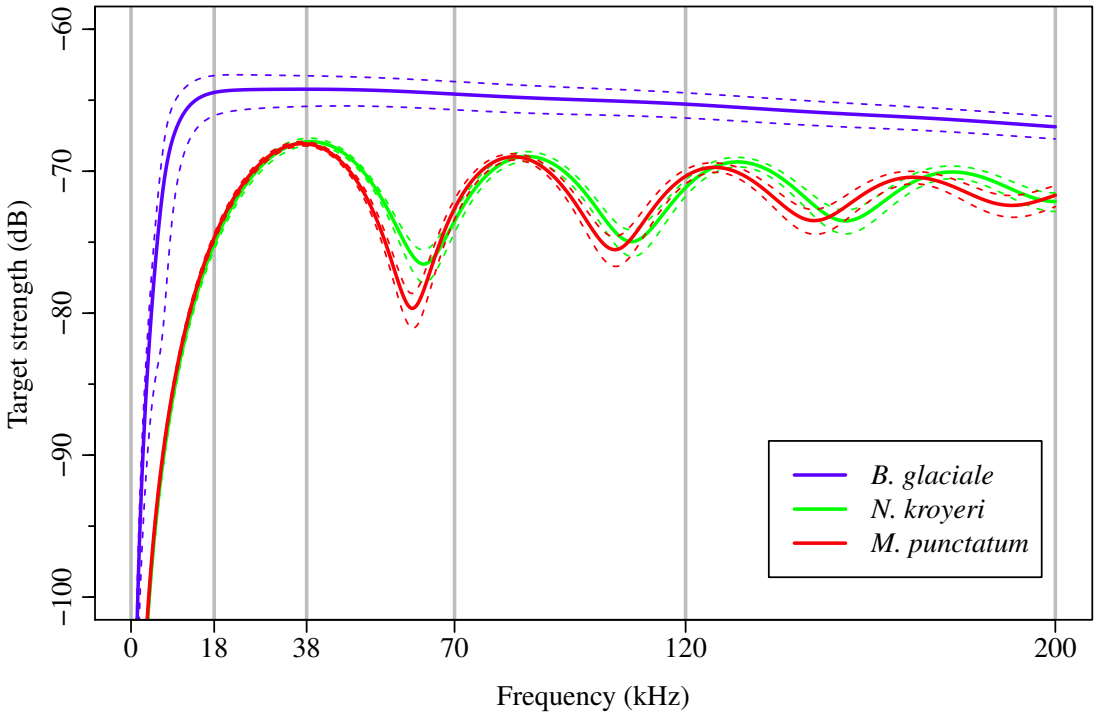

Figure 26 Comparison of the mean frequency dependence of TS estimates for *B. glaciale* (blue), *N. kroeyeri* (green) and *M. punctatum* (red). Solid lines show the mean TS of the fish at each frequency and dashed lines show corresponding 95% confidence intervals. Vertical grid lines show intersection with frequencies commonly used in scientific surveys. Estimates for N. kroeyeri and M. punctatum are based on DWBA model only while for *B. glacieale* estimates are based on combination of DWBA and RSM model results.

3.4 Target Strength length relationship

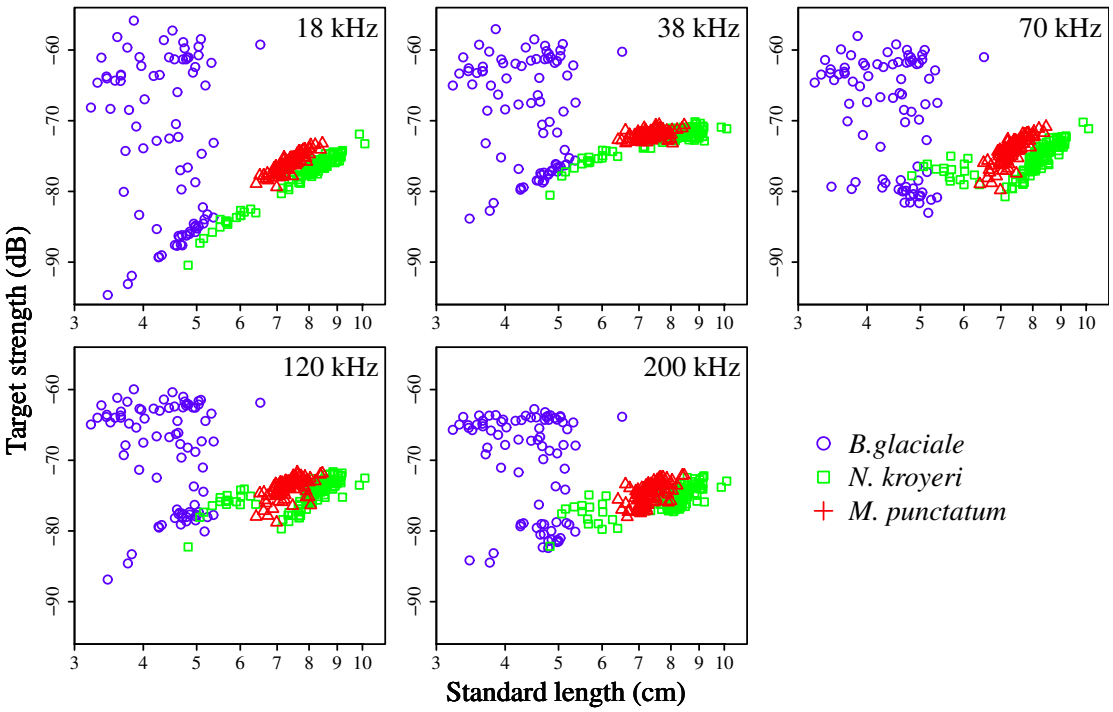

Figure 27 TS of all 3 species against log10 standard length at frequencies of 18, 38, 70, 120 and 200 kHz. *B. glaciale* (n=82), *N. kroeyeri* (n=126), and *M. punctatum* (n=99). Estimates for N. kroeyeri and M. punctatum are based on DWBA model only while for *B. glacieale* estimates are based on combination of DWBA and RSM model results.

TS of *N. kroeyeri* increased significantly (log-linear) with length at all five frequencies (Table 3 and Figure 27), and the increase was particularly pronounced at 18 and 38 kHz. TS of *M. punctatum* also increased significantly with length at all studied frequencies (Table 3 and Figure 27). In the case of *B. glaciale* the whole fish results of the two models are very scattered and show no relationship between TS and fish length (Figure 27). Hence we only comment generally about the trends in TS for mean lengths of this species with the summary statistics shown in Table 4.

3.5 Resonance

The resonance frequency of the airfilled swimbladders changes with depth.

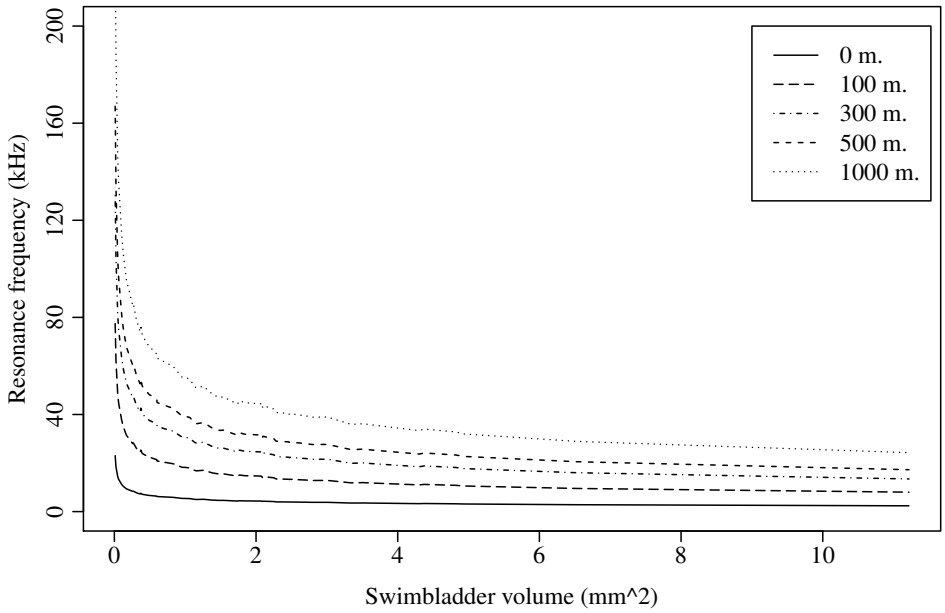

Figure 28 Resonance frequency for *B.* glaciale swimbladders as function of swimbladder volume at different depths (based on RSM model).

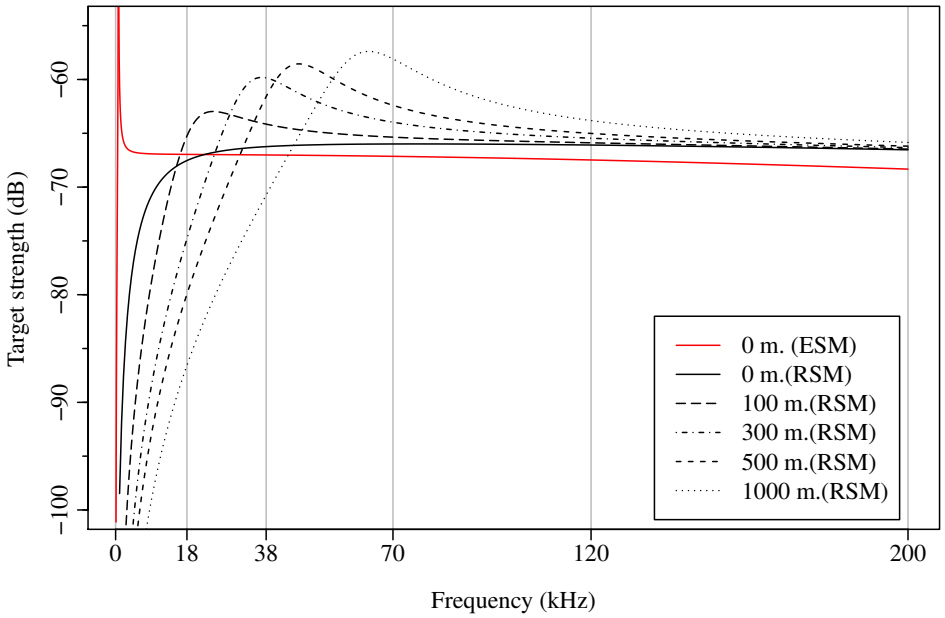

Figure 29 TS versus frequency at various depths (RSM model) compared to estimates from the exact solution model (ESM). Shown estimates are based on a swimbladder with volume of 1.16 mm^3 in 4.6 cm long *B. glaciale*.

The relation of the swimbladder volume and corresponding resonance frequency at given depths is shown in Figure 28 and the change of TS at resonance is clearly evident in Figure 29 where the shift of resonance frequency as predicted by RSM is evident along with the damping. Variability with depth becomes evident if we consider whole fish TS estimated from body (DWBA model) and swimbladder (RSM model) compared with fish length (Figure 30).

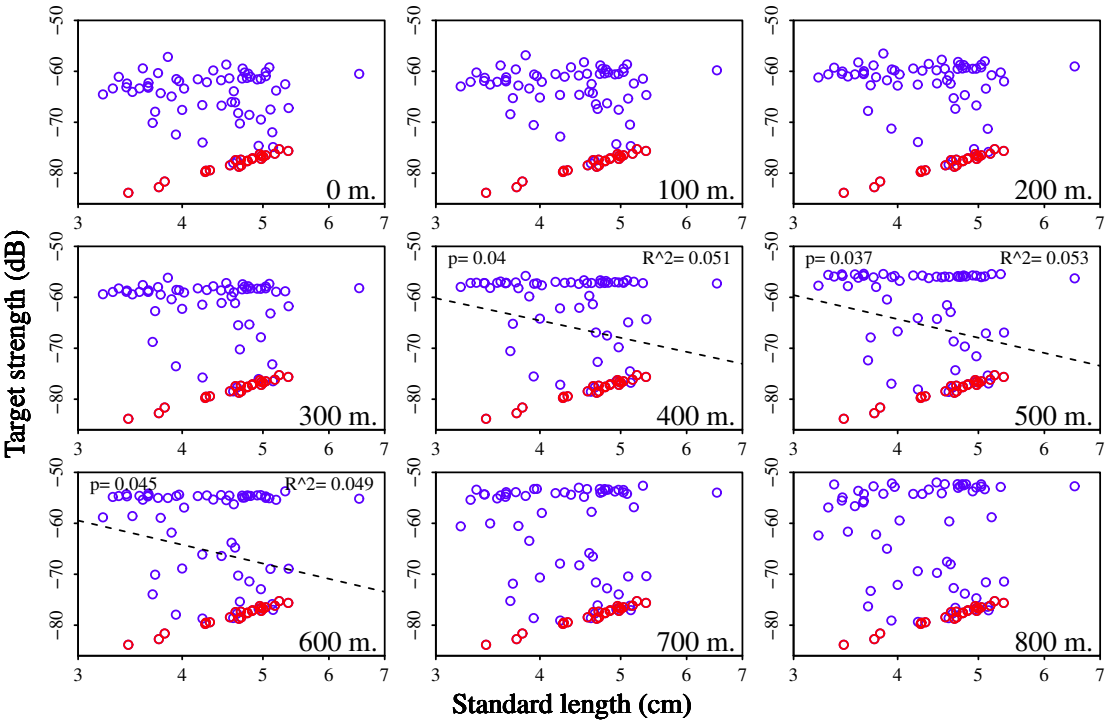

Figure 30 Whole fish TS from the sum of body (DWBA) and swimbladder (RSM) backscatter of *B. glaciale* against standard length (notice $\log_{10}$ scale on axis) at 38 kHz (n=82). Blue and red circles represent fish with and without air in the swimbladder respectively. Regression lines for all fish are shown only when slope was significant ($p<0.05$) from 0 or just above.

Further, the differences between the TS estimates from RSM and ESM models for each swimbladder mainly show the difference in resonance prediction (Figure 31).

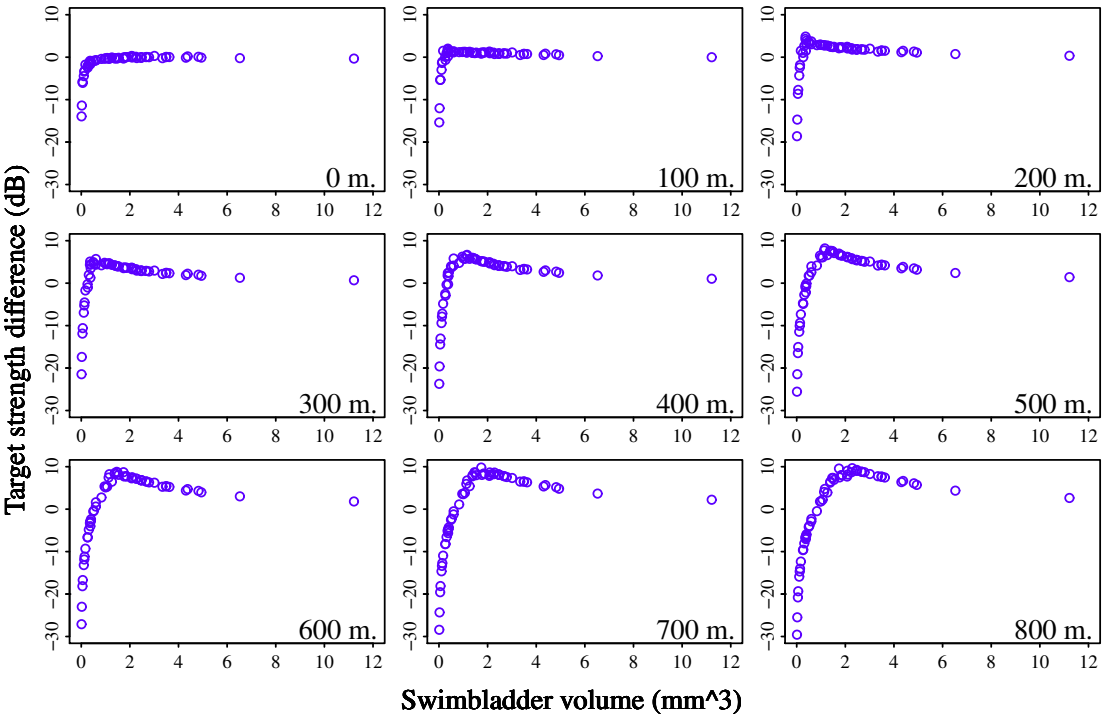

Figure 31 The difference between the RSM and ESM models in estimated TS of swimbladder ($TS_{SS} - TS_{PSM}$) versus swimbladder volume at 38 kHz. Similar pattern is evident at the other frequencies examined but the peak of resonance is at lower swimbladder volume for higher frequencies.

4 DISCUSSION

4.1 Swimbladder and morphology

This research has revealed that adult *N. kroeyeri* and *M. punctatum* in the size ranges studied here (SL; 4.8-10.1 and 6.4-8.5 cm respectively) do not have air in their swimbladders. Conversely 71% of the *B. glaciale* population (SL; 3.2-6.5 cm) has air in the swimbladder.

The negative air-bubble length versus body length relationship (Figure 21) and total lack of air in part of the *B. glaciale* population (Figure 20) is evidence of reduction of air in the swimbladder as the fish grows. Atrophy of air in the swimbladder has previously been observed in myctophids (Butler & Pearcy 1972; Yasuma *et al.* 2003; Yasuma *et al.* 2006; Yasuma *et al.* 2010), and this phenomenon is likely to be an adaptation to the pronounced diel vertical migration behaviour these fish undertake: the extensive vertical range would require considerable secretion and absorption of gas to maintain constant swimbladder volume and hence constant buoyancy (Yasuma *et al.* 2003). It remains a possibility that earlier development stages of *N. kroeyeri* and *M. punctatum* juveniles have air in their swimbladders.

4.2 Target Strength models

To estimate the TS of *B. glaciale* with air in the swimbladder we used the RSM model following Ye (1997a) and Love (1978). The prolate spheroid assumption in the model is likely to match closely the simple shape of the air-bubbles observed in swimbladders of *B. glaciale* (Figure 20). The resonance frequencies of *B. glaciale* swimbladders address the appropriate choice of acoustic frequencies for surveys of the habitat depths of *B. glaciale*. It appears from this model that *B. glaciale* is likely

to come into resonance at the lower frequencies studied here, an observation that is especially noteworthy for the commonly used 38 kHz frequency (Figure 29). Whole fish TS from the sum of body (DWBA) and swimbladder (RSM) give different TS-length distributions at different depths and frequencies. Figure 30 shows how the air filled and airless fish usually separate into two groups, although the separation varies at different depths due to resonance. The difference between swimbladder TS estimates from the two models ($TS_{RSM} - TS_{ESM}$) plotted against swimbladder volume reveals the difference of how the models predict the Rayleigh, resonance and geometric scattering (Simmonds & MacLennan 2005) with increasing swimbladder volume at each given depth. The difference between the two models can largely be explained by the resonance frequency shift and the shape effect (in the numerator of eq. 38) of the prolate spheroid in the RSM model. Further there is more constant similarity in the geometric scattering region, e.g. for larger swimbladders (Figure 31) and in single fish TS-frequency relationships (Figure 29).

To estimate the TS of the myctophid body we used the DWBA model. Thus far this model has mainly been used on zooplankton (e.g. reviewed in Stanton & Chu (2000) and Simmonds & MacLennan (2005)) as it is most appropriate for weak scatterers where mass-density and sound speed must be within 10% of corresponding values in the surrounding water. We found these contrasts (0.7% and 2.6% respectively) to be well within those limits and hence we consider the DWBA model to be suitable for the airless body components of the myctophids in this study. Equation 2 shows that the morphology of the fish and the mass-density contrast (g) and sound speed contrast (h) are important parameters for the TS of the airless fish body. This makes the physical properties of the fish body and the surrounding seawater highly important. For the myctophid *S. leucopsarus*, Yasuma *et al.* (2006) estimated g and h to be

1.002-1.019 and 1.032-1.039 respectively under expected environmental conditions. Using the same physical parameters for the myctophid body we get g=1.007 and h=1.027. Further, at the same temperature (6.4°C) our values of h are 0.9% lower than those of Yasuma *et al.* (2006) because of the different physical properties of the seawater in our study area. In the DWBA model this gives us about 2 dB lower TS estimate for a 7.9 cm long *N. kroeyeri*, highlighting the importance of correctly accounting for environmental parameters.

4.3 Target Strength

Individual *M. punctatum* show considerable variability in TS with tilt angle, and different relative positions of minimum, median and maximum TS are evident as a function of fish size. Similar trends were found for *N. kroeyeri*. The RSM derived TS tilt patterns for the swimbladder of *B. glaciale* containing air (Figure 23) show much less tilt dependence, especially at the lower frequencies. This can be explained by the rounded shape of the swimbladder and its small size compared to the wavelength of the incident wave.

N. kroeyeri and *M. punctatum* show similar patterns of TS with frequency (Figure 26). The mean TS values for *B. glaciale* in Table 4 are derived from the sum of the RSM model for swimbladder and DWBA model for body although those average values are different from the others, especially at 18, 70 and 120 kHz and Table 4 show that there will be considerable overlap of TS at all frequencies.

The two airless species *N. kroyeyri* and *M. punctatum* have very similar TS-length relationship, although *N. kroeyeri* has a slightly lower TS due to its more slender body shape. The ranges of estimated TS for *N. kroeyeri* (TS=-90 to -70 dB) at the five frequencies here examined (18, 38, 70, 120 and 200 kHz) and *M. punctatum* (TS=-80

to -72 dB) at same frequencies are quite low compared to Mamylov (1988). Although information on TS of myctophids in the north east Atlantic is very scarce, *in situ* TS estimates of myctophids in the north west Atlantic by Mamylov (1988) gave considerably higher values ranging from -60 to -52 dB at 38 kHz possibly due to air in the targeted fish species. On the other hand our results are in good agreement with Yasuma *et al.* (2006) where the airless myctophid *S. leucopsarus* in the subarctic Pacific was estimated to have TS ranging between -90 and -60 dB at four frequencies (38, 70, 120 and 200 kHz). Further, they found good agreement between their theoretical estimates and experimental measurements at 38 kHz.

Torgersen & Kaartvedt (2001) and Kaartvedt *et al.* (2009) estimated the TS of *B. glaciale* of 5.4 and 6 cm mean lengths respectively in Norwegian waters to range from about -54 to -69 dB and -52 to -62 dB (ventral aspect) respectively at 38 kHz using echo target tracking. Their estimates are rather high compared to our results for the same species (Figure 27). This difference raises the possibility that the target tracking method was missing out the *B. glaciale* of lower TS, or that there might be less of a tendency for air reduction in the swimbladders of the *B. glaciale* populations in the Norwegian fjords. Still, it should be noted that my study is solely based on theoretical models that would ideally benefit from comparison with *in situ* data and investigation of the parameters used. For an instance, the values for surface tension (s) and viscosity parameter (ξ) were simply based on notation published by Love (1978) and Love (2013), but trials (not shown in this presentation) with variable viscosity showed noteworthy difference in the damping effect.

The low TS values obtained in current study might indicate that myctophids are even more abundant in the area than has been anticipated in the past.

The myctophids are abundant oceanic pelagic fish that are one of the major components of the sound scattering layers at depths of 0 – 800 m. They are important vertically migrating zooplankton consumers in the oceanic mesopelagic ecosystem. Recently there has been considerable interest in fisheries of lanternfish. Here we present to the best of our knowledge the first length related TS estimates of those three dominant myctophid species in Irminger sea. These multifrequency TS data will assist with acoustic identification and biomass estimation of lanternfish that, in turn, will enable contribution of much-needed lanternfish data to ecosystem models.

5 FUTURE WORK

The results of this study offer an increased knowledge to examine the DSL in more detailed and quantitative manner than before. The weak scattering properties of all three species address the need for echosounders operated at short ranges, e.g. deep towed or autonomous vehicles, to overcome signal to noise ratio limitations. Further, depth related resonance properties of *B. glaciale* swimbladders suggest the use of depth stratified approach. Also the enormous effects of resonance on the frequency response of *B. glaciale* could benefit multi-frequency discrimination or even the use of broad frequency bandwidth for species discrimination or ecosystem modelling. Behavioural studies including tilt angles, vertical migrations, schooling and layer recognition are also needed. As mentioned in the discussion, this theoretical study ideally needs to be supported by *in situ* measurements, although it may be difficult to achieve representative *in situ* TS estimates of those small, weak scattering deep dwelling fish, i.e. as there might be a risk of filtering out the scatter from the weaker scattering portion of the population. Further, the assumption that the myctophid manages to maintain the volume of the physoclistous swimbladder while slowly towed from depth needs to be evaluated.

6 REFERENCES

Acevedo S., Fives J. M. 2001. The distribution and abundance of the larval stages of the myctphid *Benthosema Glaciale* (Reinhardt) in the Celtic Sea and West Coast of Ireland in 1998. Proceedings of the Royal Irish Academy, 101B:245-249

Amakasu K., Furusawa M. 2006. The target strength of Antarctic krill (Euphausia superba) measured by the split-beam method in a small tank at 70 kHz. Ices Journal Of Marine Science, 63:36-45

Anderson C. I. H., Brierley A. S., Armstrong F. 2005. Spatio-temporal variability in the distribution of epi- and meso-pelagic acoustic backscatter in the Irminger Sea, North Atlantic, with implications for predation on *Calanus finmarchicus*. Marine Biology, 146:1177-1188

Anderson V. C. 1950. Sound Scattering from a Fluid Sphere. The Journal of the Acoustical Society of America, 22:426-431

Andreeva I. B. 1964. Scattering of sound by air bladders of fish. Sov Phys Acoust, 10:17-20

Anon. 2002. Report of the Planning group on redfish stocks. ICES CM, CM 2002:1-47

Anon. 2003. Report of the Planning Group on Redfish Stocks. ICES CM, CM 2003:1-43

Backus R. H., Craddock J. E. 1977. Pelagic faunal provinces and sound-scattering levels in the Atlantic Ocean. In: Andersen NR, Zahuranec BJ (eds) Oceanic sound-scattering prediction. Plenum Press, New York, p 529-549

Backus R. H., Craddock J. E., Haedrich R. L., Robinson B. H. 1977. Atlantic Mesopelagic Zoogeography. In: Gibbs RH, Berry FH, Böhlke JE, Cohen DM, Collette BB, Eschmeyer WN, Mead GW, Merriman D, Pietsh TW (eds) Fishes of the Western North Atlantic, I, Vol 7. Sears Foundation for Marine Research, Yale University, New Haven, p 266-287

Badcock J. 1981. The significance of meristic variation in *Benthosema glaciale* (Pisces, Myctophoidei) and of the species distribution off northwest Africa. Deep Sea Research Part A Oceanographic Research Papers, 28:1477-1491

Benoit-Bird K. J., Au W. W. L. 2001. Target strength measurements of Hawaiian mesopelagic boundary community animals. The Journal of the Acoustical Society of America [HW Wilson - AST], 110:812

Benoit-Bird K. J., Au W. W. L., Kelley C. D., Taylor C. 2003. Acoustic backscattering by deepwater fish measured in situ from a manned submersible. Deep Sea Research Part I: Oceanographic Research Papers, 50:221

Bodholt H. 1991. Basic theory of underwater acoustics, Simrad

Bond C. E. 1996. Biology of fishes, Vol. Thomson Learning Inc.

Bone Q., Marshall N. B. 1982. Biology of fishes, Vol. Blackie & Son Limited, Glasgow

Borchers H. W. 2014. pracma: Practical Numerical Math Functions

Butler J. L., Pearcy W. G. 1972. Swimbladder morphology and specific gravity of Myctphids off Oregon. Journal of Fisheries Research Board of Canada, 29:1145-1150

Chu D. Z., Foote K. G., Stanton T. K. 1993. Further analysis of target strength measurements of Antarctic krill at 38 and 120 Khz - Comparison with deformed cylinder model and inference of orientation distribution. J Acoust Soc Am, 93:2985-2988

Clay C. S., Horne J. K. 1994. Acoustic models of fish: the Atlantic cod (Gadus morhua). Journal of Acoustical Society of America, 96:1661-1668

Dalpadado P., Ellertsen B., Melle W., Skjoldal H. R. 1998. Summer distribution patterns and biomass estimates of macrozooplankton and micronekton in the Nordic Seas. Sarsia, 83:103-116

Davison P. C., Checkley Jr D. M., Koslow J. A., Barlow J. 2013. Carbon export mediated by mesopelagic fishes in the northeast Pacific Ocean. Progress in Oceanography, 116:14

Doonan I. J., Bull B., Coombs R. F. 2003. Star acoustic surveys of localized fish aggregations. ICES Journal of Marine Science, 60:132

Farquhar G. B. 1977. Biological sound scattering in the oceans: A review. In: Andersen NR, Zahuranec BJ (eds) Oceanic soundscattering prediction, Vol 5. Plenum Press, New York, p 493-527

Feuillade C., Clay C. S. 1999. Anderson (1950) revisited. The Journal of the Acoustical Society of America, 106:553-564

Fock H. O., Pusch C., Ehrich S. 2004. Structure of deep-sea pelagic fish assemblages in relation to the Mid-Atlantic Ridge (45 degrees-50 degrees N). Deep-Sea Res Pt I, 51:953-978

Foote K. G. 1987. Fish Target Strengths For Use In Echo Integrator Surveys. J Acoust Soc Am, 82:981-987

Foote K. G. 1991. Summary of methods for determining fish target strength at ultrasonic frequencies. ICES Journal of Marine Science: Journal du Conseil, 48:211-217

Francois R. E., Garrison G. R. 1982a. Sound absorbtion based on ocean measurements. Part II: Boric acid contribution and equation for total absorption. J Acoust Soc Am, 72:1879ö1890

Francois R. E., Garrison G. R. 1982b. Sound absorption based on ocean measurements: Part I: Pure water and magnesium sulfate contributions. J Acoust Soc Am, 72:896-907

Furusawa M. 1988. Prolate spheroidal models for predicting general trends of fish target strength. Journal of the Acoustical Society of Japan, 9:13-24

Gauthier S., Horne J. K. 2004. Potential acoustic discrimination within boreal fish assemblages. ICES Journal of Marine Science, 61:836-845

Gjosaeter J. 1973a. Age, Growth, and Mortality of Myctophid Fish, *Benthosema glaciale* (Reinhardt), from Western Norway. Sarsia:1-14

Gjosaeter J. 1973b. The Food of Myctophid Fish, *Benthosema glaciale* (Reinhardt), from Western Norway. Sarsia:53-58

Gjosaeter J. 1978. Resource studies of mesopelagic fish. University of Bergen

Gjosaeter J. 1981a. Growth, production and reproduction of the myctophid fish, *Benthosema glaciale*, from westernNorway and adjacent seas. FiskDir Skr Ser HavUnders, 17:79-108

Gjosaeter J. 1981b. Life history and ecology of the myctophid fish *Notoscopelus elongatus* kroeyeri from the Northeast Atlantic. FiskDir Skr Ser HavUnders, 17:133-152

Gjosaeter J., Kawaguchi K. 1980. A review of the world resources of mesopelagic fish. FAO Fisheries Technical Paper, 193:1-150

Godo O. R., Patel R., Pedersen G. 2009. Diel migration and swimbladder resonance of small fish: some implications for analyses of multifrequency echo data. ICES J Mar Sci, 66:1143-1148

Gorska N., Ona E. 2003. Modelling the effect of swimbladder compression on the acoustic backscattering from herring at normal or near-normal dorsal incidences. ICES Journal of Marine Science, 60:1381

Gorska N., Ona E., Korneliussen R. 2005. Acoustic backscattering by Atlantic mackerel as being representative of fish that lack a swimbladder. Backscattering by individual fish. ICES Journal of Marine Science, 62:984-995

Halliday R. G. 1970. Growth and Vertical Distribution of Glacier Lanternfish, *Benthosema glaciale*, in Northwestern Atlantic. Journal of the Fisheries Research Board of Canada, 27:105-&

Heino M., Porteiro F. M., Sutton T. T., Falkenhaug T., Godo O. R., Piatkowski U. Catchability of pelagic trawls for sampling deep-living nekton in the mid-North Atlantic. Ices Journal Of Marine Science, 68:377-389

Hopkins T. L., Baird R. C. 1977. Aspects of the feeding ecology of oceanic midwater fishes. In: Andersen NR, Zahuranec BJ (eds) Oceanic sound scattering prediction, Vol 5. Plenum Press, New York, p 325-360

Horne J. K. 2000. Acoustic approaches to remote species identification: a review. Fisheries Oceanogr, 9:356-371

Hulley P. A. 1984. Myctophidae. In: Whitehead PJP (ed) Fishes of the North-eastern Atlantic and the Mediterranean, Vol 1. Unesco, Paris, p 429-483

Irigoien X.*, et al.* 2014. Large mesopelagic fishes biomass and trophic efficiency in the open ocean. Nat Commun, 5

Johannesson K. A., Mitson R. B. 1983. Fisheries acoustics Apractical manual for aquatic biomass estimation. FAO Fisheries Technical Paper, 240:1

Kaartvedt S., Rostad A., Klevjer T. A., Staby A. 2009. Use of bottom-mounted echo sounders in exploring behavior of mesopelagic fishes. Mar Ecol-Prog Ser, 395:109-118

Kaartvedt S., Staby A., Aksnes D. L. 2012. Efficient trawl avoidance by mesopelagic fishes causes large underestimation of their biomass. Marine Ecology Progress Series, 456:1-6

Kaartvedt S., Torgersen T., Klevjer T. A., Rostad A., Devine J. A. 2008. Behavior of individual mesopelagic fish in acoustic scattering layers of Norwegian fjords. Mar Ecol-Prog Ser, 360:201-209

Kashkin N. I. 1974. Ichthyofauna of Sound-Scattering Layers in Northeastern Atlantic. Oceanology-Ussr, 14:446-450

Kawaguchi K., Mauchline J. 1982. Biology of myctophid fishes (family Myctophidae) in the Rockall Trough, norheastern Atlantic Ocean. Biological Oceanography, 1:337-373

Kawaguchi K., Mauchline J. 1987. Biology of Sternoptychid Fishes Rockall Trough, Northeastern Atlantic Ocean. Biological Oceanography, 4:99-120

Kinzer J. 1977. Observations on feeding habits of the mesopelagic fish *Benthosema glaciale* (Myctophidae) off N. W. Africa. In: Andersen NR, Zahuranec BJ (eds) Oceanic Sound Scattering Prediction. Plenum Press, New York, p 381-392

Kinzer J. 1982. The food of four myctophid fish species off Northwest Africa. Rapp P-v Reun Cons int Explor Mer, 180:385-390

Kloser R. J., Ryan T., Sakov P., Williams A., Koslow J. A. 2002. Species identification in deep water using multiple acoustic frequencies. Can J Fish Aquat Sci, 59:1065-1077

Kloser R. J., Ryan T. E., Young J. W., Lewis M. E. 2009. Acoustic observations of micronekton fish on the scale of an ocean basin: potential and challenges. ICES J Mar Sci, 66:998-1006

Kloser R. J., Williams A., Koslow J. A. 1997. Problems with acoustic target strength measurements of a deepwater fish, orange roughy (Hoplostethus atlanticus, Collett). ICES Journal of Marine Science, 54:60-71

Koslow J. A., Kloser R. J., Williams A. 1997. Pelagic biomass and community structure over the mid-continental slope off southeastern Australia based upon acoustic and midwater trawl sampling. Mar Ecol-Prog Ser, 146:21-35

Lavery A. C., Stanton T. K., McGehee D. E., Chu D. Z. 2002. Three-dimensional modeling of acoustic backscattering from fluid-like zooplankton. J Acoust Soc Am, 111:1197-1210

Lawson G. L., Wiebe P. H., Ashjian C. J. 2006. Improved parameterization of Antarctic krill target strength models. Journal of Acoustical Society of America, 119:232-242

Lilja J., Marjomaki T. J., Jurvelius J., Rossi T., Heikkola E. 2004. Simulation and experimental measurement of side-aspect target strength of Atlantic salmon (Salmo salar) at high frequency. Can J Fish Aquat Sci, 61:2227-2236

Longhurst A. 1995. Seasonal cycles of pelagic production and consumption. Progress In Oceanography, 36:77

Longhurst A. 1998. Ecological geography of the sea, Vol. Academic Press, San Diego

Love R. H. 1978. Resonant acoustic scattering by swimbladder-bearing fish. The Journal of the Acoustical Society of America, 64:571-580

Love R. H. 2013. Response to Comment on ˜Resonant acoustic scattering by swimbladder-bearing fish"[J. Acoust. Soc. Am. 64, 571â€“580 (1978)]. The Journal of the Acoustical Society of America, 134:3399-3402

Mackenzie K. V. 1981. Nine-term equation for speed of sound in the oceans. Journal of Acoustical Society of America, 66:807-812

Magnusson J. 1996. The deep scattering layers in the Irminger Sea. Journal of Fish Biology, 49:182-192

Magnusson J., Magnusson J. V. 1995. Oceanic redfish (*Sebastes mentella*) in the Irminger Sea and adjacent waters. Sci Mar, 59:241-254

Mamylov V. S. 1988. Results of "in situ" target strength measurements at 38 kHz for major commercial species in the North Atlantic. In: Instrumental Methods of Evaluation of the Stock Size of Commercially-Important Species, Murmansk, p 3-18

Marshall N. B. 1960. Swimbladder structure of deep-sea fishes in relation to theyr systematics and biology. Discovery Reports, 31:1-122

Medwin H., Clay C. S. 1998. Fundamentals of Acoustical Oceanography, Vol. Academic Press, Boston

Nafpaktitis B. G. 1975. Review of the Lanternfish Genus *Notoscopelus* (Family Myctophidae) in North-Atlantic and Mediterranean. Bull Mar Sci, 25:75-87

Nafpaktitis B. G., Backus R. H., Craddock J. E., Haedrich R. L., Robison B. H. 1977. Family Myctophidae. In: Gibbs RH, Berry FH, Böhlke JE, Cohen DM, Collette BB, Eschmeyer WN, Mead GW, Merriman D, Pietsh TW (eds) Fishes of the Western North Atlantic, I, Vol 7. Sears Foundation for Marine Research, Yale University, New Haven, p 13-265

Nagai T. 2003. Non-destructive analysis using soft X-ray apparatuses. ESPEC Thecnology Report, 15:34-37

O'Driscoll R. L. 2003. Determining species composition in mixed-species marks: an example from the New Zealand hoki (*Macruronus novaezelandiae*) fishery. ICES Journal of Marine Science, 60:609-616

Olivar M. P., Sabates A. 1997. Vertical distribution of fish larvae in the north-west Mediterranean Sea in spring. Marine Biology, 129:289-300

Olivar M. P., Sabates A., Abello P., Garcia M. 1998. Transitory hydrographic structures and distribution of fish larvae and neustonic crustaceans in the northwestern Mediterranean. Oceanologica Acta, 21:95-104

Petitgas P., Levenez J. J. 1996. Spatial organization of pelagic fish: echogram structure, spatio-temporal condition, and biomass in Senegalese waters. ICES Journal of Marine Science, 53:147-153

R-Core-Team 2014. R: A Language and Environment for Statistical Computing. R Foundation for Statistical Computing, Vienna, Austria

Reeder D. B., Stanton T. K. 2004. Acoustic scattering by axisymmetric finite-length bodies: An extension of a two-dimensional conformal mapping method. J Acoust Soc Am, 116:729-746

Roe H. S. J., Badcock J. 1984. The Diel Migrations and Distributions within a Mesopelagic Community in the Northeast Atlantic.5. Vertical Migrations and Feeding of Fish. Progress In Oceanography, 13:389-424

Ropke A. 1989. Small-scale vertical distribution of ichthyoplankton in the Celtic Sea in April 1986. Meeresforschung-Reports on Marine Research, 32:192-203

Sabates A. 2004. Diel vertical distribution of fish larvae during the winter-mixing period in the Northwestern Mediterranean. ICES Journal of Marine Science, 61:1243

Sabates A., Bozzano A., Vallvey I. 2003a. Feeding pattern and the visual light environment in myctophid fish larvae. Journal of Fish Biology, 63:1476-1490

Sabates A., Rossi S., Reyes E. 2003b. Lipid content in the early life stages of three mesopelagic fishes. Journal of Fish Biology, 63:881-891

Sabates A., Saiz E. 2000. Intra- and interspecific variability in prey size and niche breadth of myctophiform fish larvae. Mar Ecol-Prog Ser, 201:261-271

Sameoto D. 1989. Feeding Ecology of the Lantern Fish *Benthosema glaciale* in a Subarctic Region. Polar Biol, 9:169-178

Sameoto D. D. 1988. Feeding of Lantern Fish *Benthosema glaciale* Off the Nova-Scotia Shelf. Mar Ecol-Prog Ser, 44:113-129

Sawada K., Uchikawa K., Matsuura T., Sugisaki H., Amakasu K., Abe K. 2011. In situ and ex situ target strength measurement of mesopelagic lanternfish, Diaphus theta (Family: Myctophidae). Journal of Marine Science and Technology, 19:302-311

Sawada K., Ye Z., Kieser R., McFarlane G. A., Miyanohana Y., Furusawa M. 1999. Target strength measurements and modeling of walleye pollock and Pacific hake. Fish Sci, 65:193-205

Sigurdsson T., Jonsson G., Palsson J. 2002. Deep scattering layer over Reykjanes Ridge and in the Irminger Sea. ICES CM, M:09:1-22

Simmonds E. J., MacLennan D. N. 2005. Fisheries Acoustics, Theory and Practice, Vol. Blackwell Science Ltd, London

Smith J. N., Ressler P. H., Warren J. D. A distorted wave Born approximation target strength model for Bering Sea euphausiids. Ices Journal Of Marine Science, 70:204-214

Stanton T. K. 1989. Sound scattering by cylinders of finite length. III. Deformed cylinders. The Journal of the Acoustical Society of America, 86:691-705

Stanton T. K., Chu D. 2000. Review and recommendations for the modelling of acoustic scattering by fluid-like elongated zooplankton: euphausiids and copepods. ICES Journal of Marine Science, 57:793-807

Stanton T. K., Chu D. Z., Wiebe P. H., Clay C. S. 1993. Average echoes from randomly oriented random-length finite cylinders: Zooplankton models. J Acoust Soc Am, 94:3463-3472

Suneetha K. B., Salvanes A. G. V. 2001. Population genetic structure of the glacier lanternfish, *Benthosema glaciale* (Myctophidae) in Norwegian waters. Sarsia, 86:203-212

Tåning Å. V. 1918. Mediterranean Scopelidae. Reports of the Danish Oceanographic Expedition 1908-1910, 2:1-154

Torgersen T., Kaartvedt S. 2001. In situ swimming behaviour of individual mesopelagic fish studied by split-beam echo target tracking. ICES Journal of Marine Science, 58:346-354

Urick R. J. 1967. Principles of underwater sound for engineers, Vol. McGraw-Hill, Néw York

van der Spoel S., Heyman R. P. 1983. A comparative atlas of zooplankton, Vol. Springer-Verlag, Berlin

Waterman P. C. 1969. New Formulation of Acoustic Scattering. The Journal of the Acoustical Society of America, 45:1417-1429

Weston D. E. 1967. Sound propagation in the presence of bladder fish. In: Albers VM (ed) Underwater acoustics. Plenum, New York

Yasuma H., Sawada K., Ohshima T., Miyashita K., Aoki I. 2003. Target strength of mesopelagic lanternfishes (family Myctophidae) based on swimbladder morphology. ICES Journal of Marine Science, 60:584-591

Yasuma H., Sawada K., Takao Y., Miyashita K., Aoki I. 2009. Swimbladder condition and target strength of myctophid fish in the temperate zone of the Northwest Pacific. ICES J Mar Sci, 67:135-144

Yasuma H., Sawada K., Takao Y., Miyashita K., Aoki I. 2010. Swimbladder condition and target strength of myctophid fish in the temperate zone of the Northwest Pacific. ICES J Mar Sci, 67:135-144

Yasuma H., Takao Y., Sawada K., Miyashita K., Aoki I. 2006. Target strength of the lanternfish, Stenobrachius leucopsarus (family Myctophidae), a fish without an airbladder, measured in the Bering Sea. ICES Journal of Marine Science, 63:683

Ye Z. 1997a. Low-frequency acoustic scattering by gas-filled prolate spheroids in liquids. J Acoust Soc Am, 101:1945-1952

Ye Z. 1997b. A novel approach to sound scattering by cylinders of finite length. J Acoust Soc Am, 102:877-884

Zurbrigg R. E., Scott W. B. 1972. Evidence for Expatriate Populations of Lanternfish Myctophum-Punctatum in Northwest Atlantic. Journal of the Fisheries Research Board of Canada, 29:1679-&

TABLES

Table 1 Terminalogy and values of important parameters used in the models.

Term	Symbol	Value	Units
Max. order of spherical function	m	6(PSV), 25(ESM)	
Max. degree of spherical function	n	12(PSV)	
Complex number	i	$(-1)^{1/2}$	
Sound speed in sea water	c_w	1480	m/s
Sound speed in air	c_a	330	m/s
Density of sea water	ρ_w	1027.52	Kg/m^3
Density of fish flesh	ρ_f	1035	Kg/m^3
Density of air	ρ_a	1.3	Kg/m^3
Thermal conductivity of air	κ	$5.5*10^{-3}$	cal/(m s °C)
Ratio of specific heats of air	γ	1.4	
Real part of complex shear modulus of the fish tissue	μ	10^5	Pa
Specific heat at constant pressure for air	c_{pa}	240	cal/(kg °C)
Viscosity parameter	ξ	10	kg/(m sek)
Surface tension of swimbladder	s	200	N/m

Table 2 Overview of previously published estimates of acoustic target strengths of Myctophids, where TS = m $\log_{10}$(L) + b, TS = 20 $\log_{10}$(L) + b_{20} or TS = a ln(L) + b_{ln}

Species / group	Location	Depth	Size	Swim-bladder	F (kHz)	m (dB)	b (dB)	b_{20} (dB)	a	b_{ln}	TS (dB)	Method	Ref.
Benthosema glaciale	Norway	10 - 60	5.4 cm	Yes/no	38						-54 – -69	in situ	a
Stenobrachius leucopsaurus	Alaska, Bering Sea		2.78 - 10.69 cm	no	70				32.1	-64.1		Theory + ex situ	b
Stenobrachius leucopsaurus	Alaska, Bering Sea		2.78 - 10.69 cm	no	120				16.2	-66.7		Theory + ex situ	b
Stenobrachius leucopsaurus	Alaska, Bering Sea		2.78 - 10.69 cm	no	200				12.6	-68.1		Theory + ex situ	b
Stenobrachius leucopsaurus	Alaska, Bering Sea		2.78 - 10.69 cm	no	38				15.5	-67.8		Theory + ex situ	b
Notoscopelus japonicus	Japan		12.6 - 13.3 cm	no	38			-86.7				Theory	c
Symbolophorus californiensis	Japan		8.5 - 10.8 cm	no	38			-85.7				Theory	c
Diaphus theta	Japan		2.7 - 7.7 cm	yes	200	11.8	-63.5					Theory	c
Myctophid	Hawaii		2.4 - 8.2 cm Mean = 5.1 cm		38			-58.8				ex situ	d
Mesopel. fish	Australia	0 - 100	< 3 g	yes	38						-53(-58)	in situ	e
Mesopel. Fish	Australia	0 - 100	3 - 10 g	yes	38						-49	in situ	e
Mesopel. Fish	Australia	0 - 100	> 10 g	yes	38						-42	in situ	e
Mesopel. Fish	Australia	0 - 100		no	38						-73	in situ	e
Mesopel. Fish	Australia	100 - 300	< 3 g	yes	38						-53(-58)	in situ	e
Mesopel. Fish	Australia	100 - 300	3 - 10 g	yes	38						-49(-51)	in situ	e
Mesopel. Fish	Australia	100 - 300	> 10 g	yes	38						-42	in situ	e
Mesopel. Fish	Australia	100 - 300		no	38						-71	in situ	e

a) (Torgersen & Kaartvedt 2001), b) (Yasuma *et al.* 2006), c) (Yasuma *et al.* 2003), d) (Benoit-Bird & Au 2001), e) (Koslow *et al.* 1997)

Table 2 Overview of previously published estimates of acoustic target strengths of Myctophids, where TS = m log10(L) + b, TS = 20 log10(L) + b20 or TS = a ln(L) + bln

Species / group	Location	Depth	Size	Swim-bladder	F (kHz)	m (dB)	b (dB)	b_{20} (dB)	a	b_{ln}	TS (dB)	Method	Ref.
Mesopel. Fish	Australia	300 - 525	< 3 g	yes	38						-52(-56)	in situ	e
Mesopel. Fish	Australia	300 - 525	3 - 10 g	yes	38						-49	in situ	e
Mesopel. Fish	Australia	300 - 525	> 10 g	yes	38						-42	in situ	e
Mesopel. Fish	Australia	300 - 525		no	38						-62	in situ	e
Mesopel. Fish	Australia	525 - 900	< 3 g	yes	38						-53	in situ	e
Mesopel. Fish	Australia	525 - 900	3 - 10 g	yes	38						-49	in situ	e
Mesopel. fish	Australia	525 - 900	> 10 g	yes	38						-41	in situ	e
Myctophid	NW-Atlantic		4 – 7 cm			25.2	-75					in situ	f
Ceratoscopelus warmingii	Japan		33–83	yes/no	38	26.3	-78.1						g
Ceratoscopelus warmingii	Japan		33–83	yes/no	120	26.1	-79.2						g
Myctophum asperum	Japan		31–48	yes/no	38	45.4	-88.6						g
Myctophum asperum	Japan		31–48	yes/no	120	36.3	-84.6						g
Myctophum asperum	Japan		61–77	yes/no	38	-135.2	-57.3						g
Myctophum asperum	Japan		61–77	yes/no	120	-130.8	-52.4						g
Diaphus garmani	Japan		31–57	yes/no	38	34.5	-83.5						g
Diaphus garmani	Japan		31–57	yes/no	120	32.7	-83.3						g
Ceratoscopelus warmingii	Japan		23–43	yes/no	38	49.4	-112.2						g
Ceratoscopelus warmingii	Japan		23–43	yes/no	120	10.4	-82.6						g
Myctophum asperum	Japan		18–33	yes/no	38	52.7	-108.3						g

e) (Koslow *et al.* 1997), f) (Mamylov 1988), g) (Yasuma *et al.* 2010)

Table 2 Overview of previously published estimates of acoustic target strengths of Myctophids, where TS = m log10(L) + b, TS = 20 log10(L) + b20 or TS = a ln(L) + bln

Species / group	Location	Depth	Size	Swim-bladder	F (kHz)	m (dB)	b (dB)	b_{20} (dB)	a	b_{ln}	TS (dB)	Method	Ref.
Myctophum asperum	Japan		74–86	yes/no	120	17.9	-80.9						g
Diaphus garmani	Japan		21–53	yes/no	38	54	-113.5						g
Diaphus garmani	Japan		21–53	yes/no	120	6.9	-8.4						g
Diaphus chrysorhynchus	Japan		62–100	no	38	30.5	-96.3						g
Diaphus chrysorhynchus	Japan		62–100	no	120	-9.1	-63.2						g
Diaphus theta	Japan	170-200	5.55 ± 0.43	yes	70			-70.6				in situ, ex situ, theory	h
Myctophid	Tasmania	600-1000	5.8	yes							-55		i
Myctophid	Tasmania	600-1000	9	yes							-50		i
B. glaciale	Norway		6								-52 – -62		j

g) (Yasuma *et al.* 2010), h) (Sawada *et al.* 2011), i) (Kloser *et al.* 1997), j) (Kaartvedt *et al.* 2008)

Table 3 Logarithmic (log_{10}) length dependence of TS estimated with linear regression (P-value <<0.05 in all cases). Also shown is the intersection (b_{20}) estimate from a 20 log_{10} (SL) + b_{20} regression.

Species	**Freq. (kHz)**	**TS = m log_{10} (SL) + b**	**r^2**	**n**	**b_{20}**	**r^2**
N. kroeyeri	18	48.8 log(SL) – 121.3	0.97	126	-95.5	0.62
"	38	22.6 log(SL) – 92.8	0.82	126	-90.4	0.81
"	70	20.1 log(SL) – 93.4	0.41	126	-93.3	0.40
"	120	18.0 log(SL) – 90.7	0.41	126	-92.5	0.40
"	200	17.7 log(SL) – 91.4	0.45	126	-93.4	0.43
M. punctatum	18	47.4 log(SL) – 117.2	0.76	99	-93.5	0.51
"	38	10.9 log(SL) – 81.5	0.18	99	-89.3	0.06
"	70	62.7 log(SL) – 128.5	0.65	99	-91.6	0.35
"	120	32.5 log(SL) – 102.0	0.32	99	-91.2	0.27
"	200	37.5 log(SL) – 107.2	0.35	99	-92.1	0.27

Table 4 Mean TS of *B. glaciale* and its upper and lower 95% confidence limits. Based on combined results from body (DWBA) and swimbladder (RSM) models, for fish at depth of 100 m.

Freq. (kHz)	**Mean TS**	**Lower conf.**	**Upper conf.**	**n**
18	-64.38	-65.98	-63.21	82
38	-64.29	-65.52	-63.33	82
70	-64.60	-65.71	-63.71	82
120	-65.33	-66.32	-64.52	82
200	-66.87	-67.73	-66.16	82

Table 5 Morphological measurements of *B. glaciale*.

Fish body			Swimbladder			
Length (cm)	Hight (mm)	Width (mm)	Major axis (mm)	Minor axis (mm)	Angle (°)	Volume (mm^3)
5.1	12.331	6.083	0.796	0.544	13.9	0.124
5	11.508	5.959	3.138	1.303	13.9	2.789
3.9	9.280	4.930	2.550	0.788	17.9	0.830
4.3	10.427	5.410				
3.4	8.324	3.993	3.207	1.266	9.8	2.691
4.4	10.965	5.560	3.352	1.566	18.6	4.305
5	11.805	5.862	3.204	1.158	13.2	2.250
4.6	11.218	5.545	0.475	0.302	4.0	0.023
3.2	7.756	3.952	2.120	0.929	8.2	0.958
4.7	11.338	5.421	4.101	1.428	8.8	4.375
3.8	9.478	4.803				
5.2	12.787	6.540	1.797	1.108	22.6	1.156
4.6	11.162	5.469	1.430	0.897	32.2	0.603
3.6	8.832	4.928	3.615	1.615	17.6	4.938
5.3	13.359	7.262	1.935	1.310	19.6	1.739
3.9	9.850	5.062	0.842	0.556	30.2	0.136
3.5	8.434	3.962	2.608	0.884	14.8	1.066
5.1	11.699	6.333	1.318	0.750	19.2	0.389
4.6	11.185	5.890	2.920	1.269	11.9	2.463
5.1	13.103	5.974	0.471	0.441	19.8	0.048
3.3	8.276	3.813	2.176	1.099	7.3	1.376
4.6	11.595	5.651				
4.3	10.906	5.181				
3.6	9.095	4.615	2.025	1.173	20.4	1.459
5.4	12.931	6.983	0.952	0.856	4.5	0.365
3.8	9.479	4.526	4.671	2.142	19.4	11.217
3.4	8.191	4.267	2.142	1.154	17.2	1.494
4.9	12.547	6.212	0.624	0.431	10.0	0.061
4.5	11.858	5.985	2.431	1.339	9.3	2.283
4	10.215	4.800	2.736	1.208	11.8	2.089
3.7	8.974	4.748	1.029	0.814	12.5	0.357
4.8	11.812	6.251	2.971	1.263	5.1	2.482
4.7	11.556	5.690	0.704	0.680	15.8	0.170
3.6	8.928	4.378	2.832	1.114	7.3	1.839
3.6	8.840	4.782	2.477	1.088	11.1	1.535
5	12.111	5.752	1.264	0.622	2.6	0.256
4.7	11.418	5.543				
4.9	12.403	6.286				
3.9	9.872	4.722	2.717	1.318	21.6	2.469
3.4	8.423	4.291				
4.5	11.329	5.757	3.683	1.839	12.1	6.523

Table 5 Morphological measurements of B. *glaciale*.**.**

Fish body			Swimbladder			
Length (cm)	Hight (mm)	Width (mm)	Major axis (mm)	Minor axis (mm)	Angle (°)	Volume (mm^3)
4.7	11.331	5.535	1.780	0.634	16.0	0.374
3.8	9.278	4.219	2.406	0.892	13.5	1.001
4.8	11.772	5.411	3.560	1.370	15.5	3.498
4	9.749	4.943	1.184	0.803	8.4	0.399
4.3	10.741	5.365				
4.6	11.891	5.750	1.976	1.043	15.9	1.125
3.7	9.398	4.427	1.564	0.572	12.7	0.268
4.6	11.414	5.664	1.863	0.784	10.9	0.600
3.6	9.141	4.377	2.096	1.122	8.2	1.382
3.4	8.247	4.002	2.911	1.076	23.1	1.765
4.2	10.299	5.020	0.832	0.488	7.4	0.104
3.7	9.098	4.258	3.398	1.399	12.9	3.485
4.3	10.426	5.158	2.937	1.103	8.6	1.872
4.5	11.242	5.708	1.392	0.823	17.0	0.494
4.8	12.571	5.707	3.128	1.274	0.7	2.656
5	13.044	6.522				
4.8	12.317	6.007				
3.8	9.400	4.294				
4.7	12.231	5.321				
4	10.770	4.910	2.776	0.931	15.3	1.260
4.8	11.643	5.449	3.936	1.209	16.0	3.010
5.1	13.222	7.156	4.156	1.488	22.5	4.820
4.8	11.929	5.327	1.203	0.703	22.6	0.311
5	12.965	6.009	3.502	1.406	14.7	3.623
4.7	12.273	5.752	2.894	1.270	16.3	2.445
4.8	12.625	5.926				
4.7	12.130	6.008	0.320	0.262	10.0	0.011
4.9	12.029	5.752	3.353	1.093	2.2	2.097
5.2	13.763	6.707				
4.2	11.245	5.525	3.616	1.046	12.1	2.073
4.9	12.039	6.216				
5	12.601	6.373				
4.7	12.116	6.233				
4.2	10.711	5.774	1.590	0.791	14.8	0.521
4.6	12.109	6.231				
5	12.531	6.563				
5	12.471	6.093				
5.2	13.372	7.358				
5.4	13.118	6.952				
5	11.970	6.860				
6.5	16.664	9.109	2.741	1.526	20.1	3.340

Table 6 Morphological measurements of *N. kroyeri.*

Length (cm)	Fish body Hight (cm)	Width (cm)
8.4	1.753	0.968
8.5	1.736	0.927
8.1	1.670	0.985
8.0	1.600	0.885
7.1	1.495	0.738
7.7	1.582	0.910
7.9	1.683	0.879
8.2	1.802	0.937
8.5	1.750	0.911
7.3	1.570	0.742
7.9	1.597	0.882
7.7	1.526	0.827
8.3	1.638	0.889
8.2	1.764	0.910
8.5	1.728	0.981
9.2	2.018	1.022
7.6	1.568	0.849
8.1	1.628	0.868
7.6	1.596	0.882
8.8	1.792	1.078
8.8	1.820	0.931
8.8	1.736	1.121
8.1	1.563	0.958
8.2	1.750	0.924
8.0	1.611	0.882
10.1	1.941	1.095
8.1	1.698	0.854
8.4	1.631	0.963
8.6	1.794	0.881
8.9	1.664	0.965
8.4	1.631	0.996
7.7	1.533	0.818
8.2	1.730	0.947
8.1	1.698	0.897
8.2	1.697	0.881
8.6	1.827	1.081
7.4	1.523	0.881
8.5	1.747	0.995
8.0	1.699	0.897
7.7	1.625	0.885
7.9	1.550	0.897
8.0	1.692	0.957
9.1	1.772	0.939
8.8	1.895	0.937
8.9	1.731	0.938
8.0	1.629	0.876
8.4	1.813	0.998
8.5	1.629	0.916
8.9	1.732	1.080
8.6	1.894	0.998
8.6	1.732	0.937
8.3	1.630	0.855
9.0	1.813	0.938
7.7	1.569	0.794
8.6	1.772	0.965
7.9	1.690	0.959
8.2	1.690	0.917
8.7	1.774	1.071
8.1	1.731	0.938
8.3	1.650	0.957
8.4	1.673	0.938
8.1	1.629	0.835
8.1	1.731	0.859
7.9	1.629	0.918
8.2	1.718	0.896
7.7	1.568	0.879
8.4	1.752	0.916
8.4	1.772	0.957
9.0	1.837	0.917
8.2	1.732	0.895
8.3	1.793	0.959
8.4	1.631	0.977
8.1	1.792	0.919
9.0	1.873	0.978
8.1	1.670	1.000
8.4	1.792	0.931
8.2	1.691	0.940
8.4	1.692	0.938
8.0	1.651	1.018
7.2	1.573	0.774
7.9	1.629	0.896
8.2	1.630	0.939
7.9	1.676	0.958
9.0	1.879	1.039
9.0	1.874	0.978
8.6	1.743	0.958
8.6	1.588	0.957
9.1	1.873	0.958
8.3	1.752	0.920
8.4	1.674	0.938

Table 6 Morphological measurements of N. *kroyeri.*

Length (cm)	Fish body Hight (cm)	Width (cm)
7.9	1.645	0.900
8.5	1.660	0.915
7.3	1.435	0.830
8.1	1.723	0.915
8.5	1.759	1.013
8.1	1.748	1.043
7.9	1.606	0.886
9.1	1.845	1.041
8.5	1.844	0.999
8.1	1.677	0.971
9.1	1.844	1.041
8.6	1.747	0.998
8.3	1.801	0.971
8.8	1.958	1.027
9.0	1.718	1.069
9.2	1.826	1.069
5.7	1.145	0.663
6.4	1.267	0.668
6.0	1.184	0.774
6.0	1.258	0.677
5.9	1.226	0.679
6.3	1.240	0.735
5.5	1.126	0.661
6.0	1.193	0.707
5.1	1.028	0.591
5.7	1.211	0.652
6.1	1.145	0.766
5.6	1.201	0.676
5.3	1.104	0.634
5.5	1.182	0.717
4.8	0.943	0.465
7.4	1.553	0.888
5.1	1.041	0.623
5.7	1.087	0.731
7.7	1.554	0.985
9.9	2.043	1.266
9.1	1.730	1.024

Table 7 Morphological measurements of *M. punctatum*.

Length (cm)	Fish body Length (cm)	Length (cm)	Length (cm)	Fish body Length (cm)	Length (cm)
7.7	1.838	1.036	7.6	1.864	1.063
7.5	1.845	1.094	7.8	1.839	1.079
7.3	1.807	1.044	6.6	1.750	0.938
7.4	1.816	1.010	6.9	1.571	0.954
7.3	1.783	1.020	7.0	1.681	0.945
7.4	1.712	1.052	7.7	1.876	1.179
7.5	1.590	0.907	7.1	1.673	0.966
8.0	1.906	1.094	7.0	1.696	0.952
7.2	1.628	0.944	6.9	1.806	0.997
7.4	1.861	1.069	7.1	1.767	0.995
7.2	1.640	1.035	7.2	1.711	0.884
7.3	1.749	1.044	7.0	1.638	0.910
7.1	1.799	1.044	7.9	2.016	1.123
7.9	1.945	1.035	7.1	1.779	0.994
7.4	1.895	1.094	6.9	1.738	0.994
7.5	1.837	1.111	7.4	1.811	1.036
7.1	1.707	1.014	6.7	1.626	0.938
7.4	1.728	1.019	7.1	1.667	0.972
7.5	1.845	1.069	6.7	1.652	0.996
7.2	1.630	0.910	6.4	1.554	0.914
7.9	1.974	1.179	7.1	1.792	1.039
7.5	1.765	1.135	8.0	2.030	1.162
8.2	1.961	1.232	7.6	1.820	1.064
7.3	1.835	1.075	6.9	1.778	0.981
7.1	1.764	1.047	7.3	1.848	1.022
7.0	1.656	1.008	8.1	2.118	1.198
7.5	1.639	1.064	7.6	1.766	1.023
8.4	1.876	1.153	7.3	1.694	1.008
8.0	1.918	1.190	7.0	1.764	0.938
7.6	1.778	1.191	7.2	1.736	0.994
7.0	1.639	0.995	7.4	1.752	1.036
7.4	1.814	1.051	7.0	1.766	1.038
7.6	1.834	1.115	7.1	1.780	0.938
7.2	1.694	1.064	7.3	1.797	0.980
7.2	1.904	1.123	7.5	1.723	1.149
7.6	1.820	1.155	7.3	1.750	0.952
7.7	1.885	1.190	6.6	1.517	1.037
7.2	1.668	1.005	7.4	1.904	1.041
7.0	1.708	0.925	7.5	1.709	1.078
7.5	1.890	1.053	7.8	1.904	1.101
7.2	1.807	1.065	7.2	1.652	1.087
7.1	1.680	1.016	7.0	1.652	1.036
7.0	1.498	0.832	7.6	1.768	0.996
7.2	1.905	1.078	6.5	1.709	0.968
8.5	1.918	1.252	7.8	1.960	1.176
7.6	1.890	1.070	7.5	1.695	1.093
7.4	1.751	1.050	7.9	1.765	1.022
7.0	1.796	1.028	7.9	1.848	1.120
7.1	1.695	0.927	6.7	1.511	0.950
6.7	1.667	0.910			